

**ESTIMATION OF THE RELEASE AND MIGRATION OF LEAD THROUGH SOILS  
AND GROUNDWATER AT THE HANFORD SITE 218-E-12B BURIAL GROUND**

**VOLUME 1: FINAL REPORT**

**K. Rhoads**

**B. N. Bjornstad**

**R. E. Lewis**

**S. S. Teel**

**K. J. Cantrell**

**R. J. Serne**

**J. L. Smoot**

**C. T. Kincaid**

**S. K. Wurstner**

**October 1992**

**Prepared for  
the U.S. Department of Energy  
under Contract DE-AC06-76RLO 1830**

**Pacific Northwest Laboratory  
Richland, Washington 99352**

ESTIMATION OF THE RELEASE AND MIGRATION OF LEAD THROUGH SOILS AND GROUNDWATER AT THE HANFORD SITE 218-E-12B BURIAL GROUND  
**MASTER**

## ABSTRACT

This study was performed to evaluate the potential for transport of lead from the Hanford Site 218-E-12B Burial Ground to the surrounding surface- and groundwater. Burial of metal components containing nickel alloy steel and lead at this location may eventually result in release of lead to the subsurface environment, including groundwater aquifers that may be used for domestic and agricultural purposes in the future and, ultimately, to the Columbia River.

The rate at which lead is transported to downgradient locations depends on a complex set of factors, such as climate, soil and groundwater chemistry, and the geologic and hydrologic configuration of the subsurface region between the burial ground and a potential receptor location. The geologic structure of the sedimentary formation in this area was investigated by using available published information and by observing the walls of the excavated burial trench and drilling cores taken in the region. Physical, hydraulic, and geochemical properties of the sedimentary deposits were determined by laboratory analysis of samples taken from the trench walls and a limited number of samples from drilling cores. Laboratory studies of the geochemical environment were designed to evaluate the solubility of lead compounds in Hanford groundwater and their adsorption on subsurface soils.

The groundwater transport analysis was conducted using a one-dimensional screening model with a relatively conservative matrix of parameters obtained from the hydrogeologic and geochemical studies. The predicted peak groundwater concentrations for a single component buried at this location ranged from 0.07 to 7.6  $\mu\text{g/L}$ ; those for an array of 120 components were between 0.39 and 43  $\mu\text{g/L}$ , depending on assumptions about climate and other transport parameters. The estimated transfer of lead to the Columbia River was less than 1 kg/yr in all cases, resulting in surface-water concentrations that were below 10  $\mu\text{g/L}$ . The times required to reach the peak lead concentrations in groundwater and the river ranged from 0.24 to 86 million years -- well beyond the time period over which the site is expected to retain its current geological and hydrological configuration.

## EXECUTIVE SUMMARY

An assessment was performed to evaluate release and transport of lead from large metal components containing nickel alloy steel and lead at the Hanford Site 218-E-12B Burial Ground. The potential for lead within the disposal units to enter groundwater under the burial site was investigated by examining available data on the site's geology, geochemistry, and geohydrology to develop a conceptual model for release and transport of lead from the components. In addition, laboratory studies were performed to provide information needed for the model, but which was not available from existing databases. Estimates of future concentrations of lead in groundwater and in the Columbia River were developed based on this information.

The geological strata underlying the burial ground form a sedimentary deposit known as the Hanford formation, a heterogeneous structure that contains layers ranging from fine-grained sand, clay, and silt to gravel and boulders. Beneath the Hanford formation is an extensive, relatively impermeable basalt formation that constitutes the bottom of the unconfined aquifer. Water is assumed to percolate downward through the burial site and the underlying layers of sedimentary deposits until it encounters the unconfined aquifer approximately 61 m (200 ft) below the surface. After the soil water reaches the unconfined aquifer, it is transported by groundwater flow within the aquifer, which eventually discharges to the Columbia River.

The physical and hydraulic properties of soil determine the rate at which rainwater on the surface is transported downward toward the unconfined aquifer, and they also influence the rates of competing rainwater disposition processes such as evaporation. The characteristics of the Hanford formation beneath the burial site were investigated using a number of existing resources, and by sampling soil from the excavated faces of the burial pit. Strata in the faces of the pit were mapped, and drilling logs from boreholes and wells adjacent to the burial site were used to map soil in the strata between the floor of the pit and the basalt formation. Soil samples collected at the burial pit and a limited number of samples from borehole cuttings were tested to determine their physical and hydraulic properties, including grain size distribution, moisture content, porosity, permeability, and bulk density.

The results of these tests were then used to predict the properties of similar formations in the deeper strata, and ultimately the travel time required for water to reach the unconfined aquifer.

The chemistry of soil and groundwater also play an important role in predicting transport of lead from the burial site. The release rate of lead from the metal components depends largely upon the oxidation rate of metallic lead, on the dissolution of secondary minerals such as lead carbonates in water percolating through the soil, and on the total quantity of water percolating through the soil surrounding the components. After dissolution, transport of lead from the burial ground to the aquifer below is strongly influenced by the ability of surrounding soil to adsorb and retain it. The extent to which dissolved lead is adsorbed onto soil particles is a relatively complex function of the water and soil chemistry, and of the properties of the lead species in solution. For this evaluation, soil samples from the burial site were analyzed to determine their chemical and mineralogical make-up, and the chemistry of groundwater in the vicinity was available from data taken at onsite monitoring wells.

The solubility of lead in Hanford soils and groundwater was predicted using the MINTEQ computer code along with laboratory analytical data for groundwater chemistry at an onsite monitoring well. The model predictions were then compared with the results of laboratory studies in which the solubility of lead in Hanford soil and groundwater systems were determined empirically. The results of empirical laboratory experiments, in which lead solubility was determined to be approximately 236  $\mu\text{g/L}$ , was very close to the predicted solubility of 287  $\mu\text{g/L}$  from the computer model. Because possible interactions of lead with other metals in the components were of interest, the solubility of nickel was also predicted, using the MINTEQ code, to be 16.6 mg/L. For the transport modeling, it was conservatively assumed that all water leaching from the burial ground dissolved lead and nickel compounds up to the saturation limit. Two solubility estimates for lead, 300 and 550  $\mu\text{g/L}$ , were used in the transport modeling to represent a "best estimate" and a "conservative" case.

Adsorption of lead onto soil from the burial site was being investigated using two methodologies. In batch adsorption tests, measured quantities of

soil were placed into contact with lead solution of known concentration for a variable length of time, and the distribution coefficient was determined from the relative amounts of lead remaining in solution and adsorbed to the soil at the end of the contact period. Adsorption was also measured in a dynamic flow-through column test system to more accurately simulate actual conditions at the burial site and to confirm the results of batch tests. Based on the results of batch experiments, two values of the distribution coefficient for lead, 10,000 and 1200 mL/g, were recommended for use in the transport modeling to represent the "best estimate" and "conservative" cases, respectively.

Because a substantial quantity of nickel is present in alloy steel components within the waste disposal units, the potential for nickel leaching from the components to tie up adsorption sites in the soil and interfere with adsorption of lead was investigated. This possibility was considered because reduced adsorption of lead in the soil would result in accelerated transport to downgradient groundwater locations. Iron and chromium are also significant constituents in the waste; however, these metals are not expected to influence lead transport because neither is sufficiently soluble in a chemical form that could compete with lead for soil adsorption sites. In order to determine the extent of any interaction between lead and nickel in the Hanford soil and groundwater system, additional batch adsorption experiments for lead were conducted in the presence of dissolved nickel. The distribution coefficients for lead resulting from these experiments were virtually identical to those from experiments where nickel was not present, and it was concluded that nickel in the waste components would not be likely to affect lead transport in this geologic system.

Transport modeling for this assessment utilized data on soil properties, predicted solubility, and estimates for adsorption of lead under the geochemical conditions at the burial site as described previously. The calculations also included three source terms consisting of a single waste disposal unit and arrays of 120 units having either "maximum" or "average" mass. Modeling of water flow from the burial site through the vadose zone to the unconfined aquifer included scenarios for three different recharge rates, which were coupled to a groundwater flow model appropriate to each case. A recharge rate of 0.1 cm/yr through the vadose zone was used to represent a

situation in which the burial site is protected by an engineered barrier; a recharge rate of 0.5 cm/yr was used to model an unprotected burial site under arid climatic conditions such as those that currently exist; and a recharge rate of 6.0 cm/yr was used to evaluate the potential effect of a more humid climate on lead transport from an unprotected burial site in the future.

The concentration of lead in groundwater was evaluated at two downgradient locations, 100 m and 5000 m from the burial site, and the quantity of lead entering the Columbia River annually was also estimated for the "best estimate" and "conservative" transport cases. Peak lead concentrations at the 5000-m downgradient well ranged from 0.07 to 43  $\mu\text{g/L}$  (ppb), and those at the 100-m well were comparable. The maximum annual release of lead to the Columbia River was less than 1 kg, resulting in an average concentration of  $9.2 \times 10^{-9}$  mg/L in river water. The combination of a high recharge rate with a full array source term and "conservative" transport parameters produced the highest concentrations, whereas the 0.1-cm/yr recharge rate, a single unit source term, and "best estimate" transport parameters resulted in the lowest concentrations. Even for the "conservative" case, lead was not predicted to reach the unconfined aquifer until 240,000 yr after disposal -- well beyond the time period over which the burial site is expected to retain its current geological and hydrological configuration.

## ACKNOWLEDGMENTS

The authors gratefully acknowledge the excellent secretarial support provided by Ms. D. J. McInturff, and the expert technical contributions of Ms. P. R. Heller, Ms. V. L. Legore and Mr. C. W. Lindenmeier. Special thanks to Mr. A. K. Lewis (Kaiser Engineers Hanford Co.) for providing a topographic map of the study area.

## CONTENTS

ABSTRACT . . . . .	iii
EXECUTIVE SUMMARY . . . . .	v
ACKNOWLEDGMENTS . . . . .	ix
FIGURES . . . . .	xiii
TABLES . . . . .	xiv
1.0 INTRODUCTION . . . . .	1.1
2.0 THE STRATIGRAPHY, GEOHYDROLOGIC PROPERTIES, AND SUBSURFACE FLOW CONCEPTUAL MODEL OF THE GEOHYDROLOGIC SYSTEM UNDERLYING THE 218-E-12B BURIAL GROUND . . . . .	2.1
2.1 STRATIGRAPHY . . . . .	2.1
2.2 PHYSICAL PROPERTIES OF THE HANFORD FORMATION . . . . .	2.4
2.3 HYDROLOGY . . . . .	2.6
3.0 GEOCHEMISTRY OF LEAD IN SOIL/GROUNDWATER SYSTEMS AT THE HANFORD SITE . . . . .	3.1
3.1 METHODS FOR DETERMINING LEAD AND NICKEL SOLUBILITY . . . . .	3.1
3.2 DESCRIPTION OF ADSORPTION EXPERIMENTS . . . . .	3.2
3.2.1 Preparation and Analysis of Hanford Sediment Samples . . . . .	3.4
3.2.2 Batch Adsorption Tests . . . . .	3.4
3.2.3 Column Adsorption Tests . . . . .	3.6
3.3 RESULTS AND DISCUSSION . . . . .	3.7
3.3.1 Sediment Characterization . . . . .	3.7
3.3.2 Solubility of Lead and Nickel . . . . .	3.10
3.3.3 Batch Adsorption Studies . . . . .	3.11
3.3.4 Column Adsorption Study . . . . .	3.16
3.4 DISCUSSION AND RECOMMENDATIONS FOR TRANSPORT MODELING . . . . .	3.19
4.0 WATER FLOW AND TRANSPORT OF LEAD IN HANFORD SOILS AND GROUNDWATER . . . . .	4.1
4.1 ONE-DIMENSIONAL STREAMTUBE APPROACH . . . . .	4.3
4.2 VADOSE ZONE WATER FLOW . . . . .	4.4
4.3 GROUNDWATER FLOW MODELING . . . . .	4.8
4.3.1 Groundwater Travel Times . . . . .	4.9
4.3.2 Groundwater Velocity . . . . .	4.14
4.3.3 Limitations of the CFEST Groundwater Flow Model . . . . .	4.15
4.4 LEAD TRANSPORT . . . . .	4.16
4.5 LEAD CONCENTRATIONS . . . . .	4.19
4.6 DISCUSSION . . . . .	4.25
4.7 SOURCES OF CONSERVATISM IN THE GROUNDWATER AND TRANSPORT MODELS . . . . .	4.28
4.7.1 Infiltrating Water at the Solubility Limit of Lead . . . . .	4.28
4.7.2 Hydraulic Impact of a Resource Conservation and Recovery Act Barrier . . . . .	4.28

4.7.3	Recharge Rate with a Protective Barrier . . . . .	4.29
4.7.4	Omission of Lateral or Transverse Dispersion . . . . .	4.30
4.7.5	Areal Extent of Basalt and Ringold Formation Above the Water Table . . . . .	4.31
4.7.6	Estimates of the Distribution or Adsorption Coefficient	4.32
4.8	SUMMARY . . . . .	4.33
5.0	REFERENCES . . . . .	5.1

## FIGURES

2.1.	Location Map of the 218-E-12B Burial Ground Study Area . . . . .	2.2
2.2.	Hydrogeologic Cross Section Beneath the 218-E-12B Burial Ground . .	2.3
2.3.	Presumed Groundwater Gradients and Flow Directions in the Unconfined Aquifer Beneath the Hanford Site 200 Areas . . . . .	2.8
2.4.	Water Table Contours for the Steady-State 0.5 cm/yr Recharge Case .	2.9
2.5.	Water Table Contours for the Steady-State 5.0 cm/yr Recharge Case .	2.10
3.1.	Distribution Coefficients for Lead from Radiotracer Experiments, 7- to 10-Day Equilibration Period . . . . .	3.12
3.2.	Lead Adsorption Isotherm from Radiotracer Experiments, 7- to 10- Day Equilibration Period . . . . .	3.12
3.3.	Distribution Coefficients for Lead from Radiotracer Experiments, Comparison of Values for 7- to 30-day Tests . . . . .	3.13
3.4.	Distribution Coefficients for Lead from Experiments Without Radioactive Tracer . . . . .	3.13
3.5.	Lead Adsorption Isotherm from Experiments Without Radioactive Tracer . . . . .	3.14
3.6.	Distribution Coefficients for Lead Experiments with Radioactive Tracer, Including Values Determined Near the Solubility Limit of Lead . . . . .	3.17
3.7.	Lead Distribution Coefficient as a Function of Added Calcite . . .	3.17
3.8.	Results of Lead Column Adsorption Experiments . . . . .	3.18
4.1.	Moisture Retention Curves for Soil Samples from Well 239-E33-30 . .	4.8
4.2.	Streamlines from the 218-E-12B Burial Ground to the River for the 5.0 cm/yr Site-Wide Recharge Case . . . . .	4.11
4.3.	Streamlines from the 218-E-12B Burial Ground to the River for the 0.5-cm/yr Site-Wide Recharge Case . . . . .	4.12
4.4.	Concentration of Lead in Groundwater at the 100-m Well -- Maximum Single Disposal Unit, "Conservative" Transport Case, 6-cm/yr Recharge . . . . .	4.22

4.5.	Concentration of Lead in Groundwater at the 100-m Well -- Maximum Array of Disposal Units, "Conservative" Transport Case, 0.1-cm/yr Recharge . . . . .	4.23
4.6.	Concentration of Lead in Groundwater at the 100-m Well -- Maximum Array of Disposal Units, "Conservative" Transport Case, 0.5-cm/yr Recharge . . . . .	4.23
4.7.	Concentration of Lead in Groundwater at the 100-m Well -- Maximum Array of Disposal Units, "Conservative" Transport Case, 6-cm/yr Recharge . . . . .	4.24
4.8.	Concentration of Lead in Groundwater at the 100-m Well -- Average Array of Disposal Units, "Conservative" Transport Case, 6-cm/yr Recharge . . . . .	4.24

## TABLES

2.1.	Physical and Hydraulic Properties of Hanford Formation Sediments in the Vicinity of the 218-E-12B Burial Ground . . . . .	2.5
3.1.	Chemical Composition of Hanford Groundwater <sup>(a)</sup> (Well 6-S3-25) That Was Input to MINTEQ Computer Code for Determination of Solubility for Lead and Nickel Compounds . . . . .	3.3
3.2.	Particle Size Distribution of Hanford Formation Sediments in the Vicinity of the 218-E-12B Burial Ground . . . . .	3.8
3.3.	Saturation Paste pH and Composition of Soil from the 218-E-12B Burial Ground . . . . .	3.8
3.4.	Amorphous Oxide, Calcium Carbonate and Organic Carbon Content of the "Fines" in Soil from the 218-E-12B Burial Ground . . . . .	3.9
3.5.	Exchangeable Cations and Total Cation Exchange Capacity for Soil from the 218-E-12B Burial Ground . . . . .	3.9
3.6.	Mineral Content of the Clay Size Fraction of the "Fines" Used in Adsorption Experiments . . . . .	3.9
3.7.	Solubility, Distribution Coefficient ( $R_d$ ), and Retardation Factor ( $R_f$ ) Values Recommended for Use in Transport Modeling . . . . .	3.19
4.1.	Volumetric Water Content, Pore-Water Velocity, and Water Travel Time for Three Recharge Rates Through the Burial Ground . . . . .	4.7
4.2.	Travel Times Along Individual Streamlines in the Unconfined Aquifer for the 5.0-cm/yr Site-Wide Recharge Case . . . . .	4.13
4.3.	Travel Times Along Individual Streamlines in the Unconfined Aquifer . . . . .	4.14
4.4.	Annual Flux of Lead into the Soil Column Beneath the 218-E-12B Burial Ground . . . . .	4.18
4.5.	Total Estimated Release Times for Lead from Components Disposed at the 218-E-12B Burial Ground . . . . .	4.18
4.6.	Peak Lead Concentration in Downgradient Groundwater Wells or Maximum Flux of Lead to the Columbia River as a Function of Release Conditions from the 218-E-12B Burial Ground . . . . .	4.20
4.7.	Time of Peak Lead Concentration in Downgradient Groundwater Wells or Maximum Flux of Lead to the Columbia River as a Function of Release Conditions from the 218-E-12B Burial Ground . . . . .	4.21

## 1.0 INTRODUCTION

This study was performed at Pacific Northwest Laboratory<sup>1</sup> to provide an initial estimate of lead releases to groundwater associated with the permanent disposal of large carbon steel components containing nickel alloy steel and lead at the Hanford Site 218-E-12B Burial Ground. Previous analyses for shallow waste disposal sites at Hanford (U.S. Department of Energy [DOE] 1987) indicated that use of groundwater from a downgradient well to maintain a two-hectare family farm resulted in the maximum individual exposure to radionuclides. Intrusion scenarios were not explicitly included in this analysis because the probability of direct intrusion into a waste site, and the resulting consequences for an affected individual, were generally lower than for the family farm scenario. In addition, current federal regulations for lead in the environment do not require evaluation of intruder scenarios, nor do they specify standards for media other than air and drinking water; hence, transport of lead to surface- and groundwater was considered to be the most significant benchmark for this analysis.

Estimates of lead migration in groundwater required information concerning the geologic structure underlying the burial trench, the geochemical properties of the soil/groundwater system, and the physical-hydraulic properties of the site. This study was divided into three technical tasks as follows:

- characterization of the geologic structure and physical-hydraulic properties of soil strata underlying the burial site
- characterization of the geochemical system for release and migration of lead from the disposal site, including potential competitive effects of nickel on soil adsorption of lead
- modeling of water flow and lead migration in soils and groundwater to determine future concentrations in surface- and groundwater at downgradient locations.

---

<sup>1</sup> Pacific Northwest Laboratory is operated for the U.S. Department of Energy by Battelle Memorial Institute under Contract DE-AC06-76RLO 1830.

Information needed to perform the assessment was obtained from existing literature and databases where possible, and laboratory studies were conducted to provide data that were not available from other sources. Methods used to obtain necessary data and the results of the transport analysis are described in the following sections.

## 2.0 THE STRATIGRAPHY, GEOHYDROLOGIC PROPERTIES, AND SUBSURFACE FLOW CONCEPTUAL MODEL OF THE GEOHYDROLOGIC SYSTEM UNDERLYING THE 218-E-12B BURIAL GROUND

This section of the report describes the geologic and hydrologic characteristics of the 218-E-12B Burial Ground, which is located in the 200-East area of the Hanford Site (Figure 2.1). The suprabasalt geohydrology in the vicinity of the burial ground consists of unsaturated and saturated flow within the unconsolidated sediments of the Hanford formation. In general, the Hanford formation in the vicinity of the burial ground is characterized by a relatively thick (up to 100 m) unsaturated zone and thin (0 to 10s of meters) saturated zone. The general stratigraphy of the area is discussed in this section, followed by a description of an existing conceptual model for the movement of water through this geohydrologic system. A more detailed description of the burial ground geology is presented in Appendix A.

### 2.1 STRATIGRAPHY

Three principal stratigraphic units are present beneath the 218-E-12B Burial Ground (from oldest to youngest): 1) the Miocene Columbia River basalt, interbedded with 2) sedimentary deposits of the Ellensburg Formation, and 3) the glaciofluvial Hanford formation (Last et al. 1989). The Hanford formation (informal name) makes up the vadose zone and the unconfined aquifer directly beneath the 218-E-12B Burial Ground. The Hanford formation is the principal post-basalt sedimentary unit beneath the burial ground, where it averages about 61 m in thickness (Figure 2.2). The Hanford formation was deposited during periods of cataclysmic flooding, which occurred intermittently during the last ice age (Pleistocene Epoch). The last flood event took place approximately 13,000 yr ago (Mullineaux et al. 1978).

The Hanford formation is divided into three sediment types, principally on the basis of texture: 1) gravel dominated, 2) sand dominated, and 3) silt dominated (Figure 2.2). Although all three sediment types are present within the 218-E-12B Burial Ground, the gravel-dominated sediments predominate. Heterogeneity among these sediment types within the Hanford formation occurs at such a scale that strata identified in one borehole often cannot be

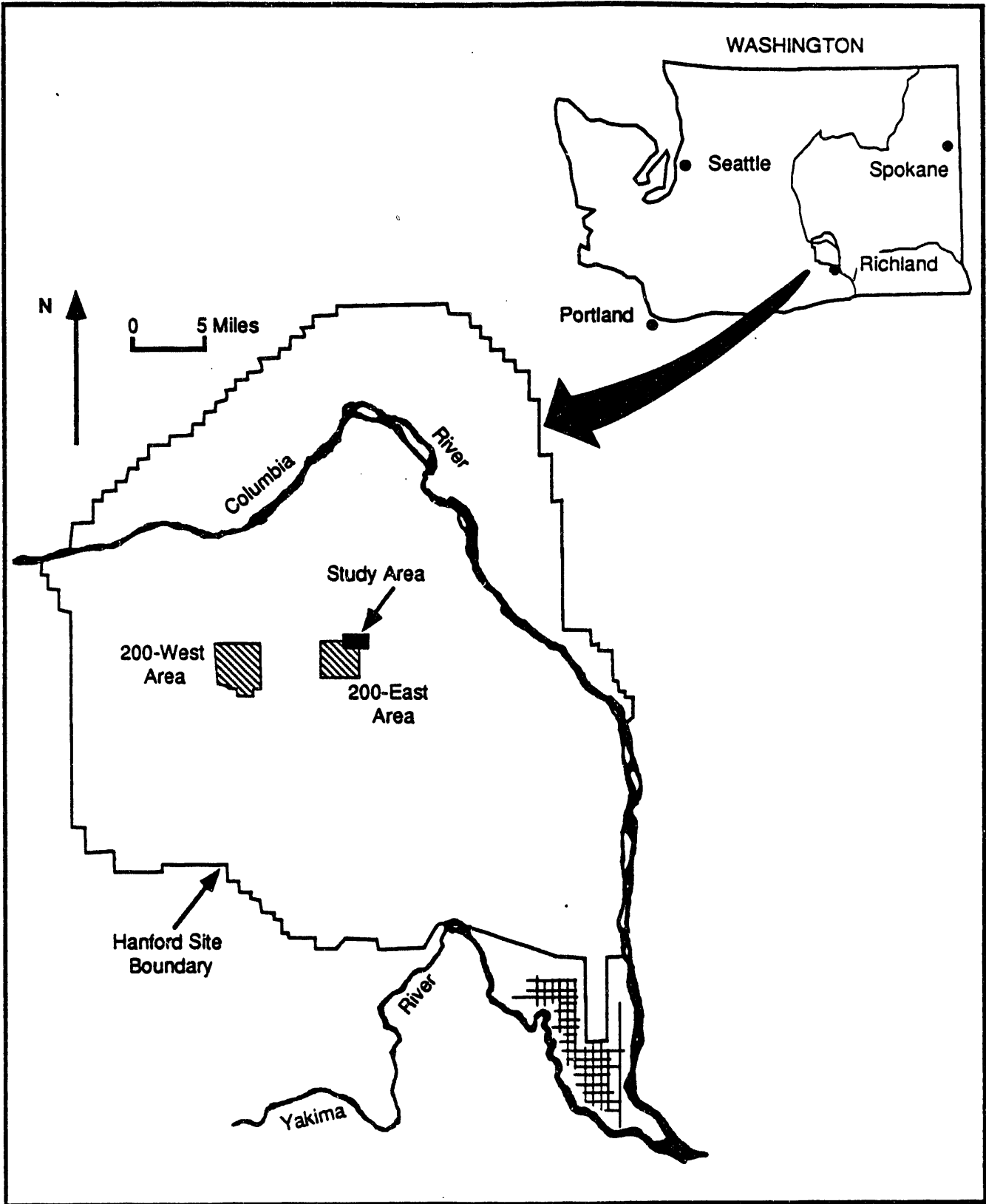


**FIGURE 2.1.** Location Map of the 218-E-12B Burial Ground Study Area

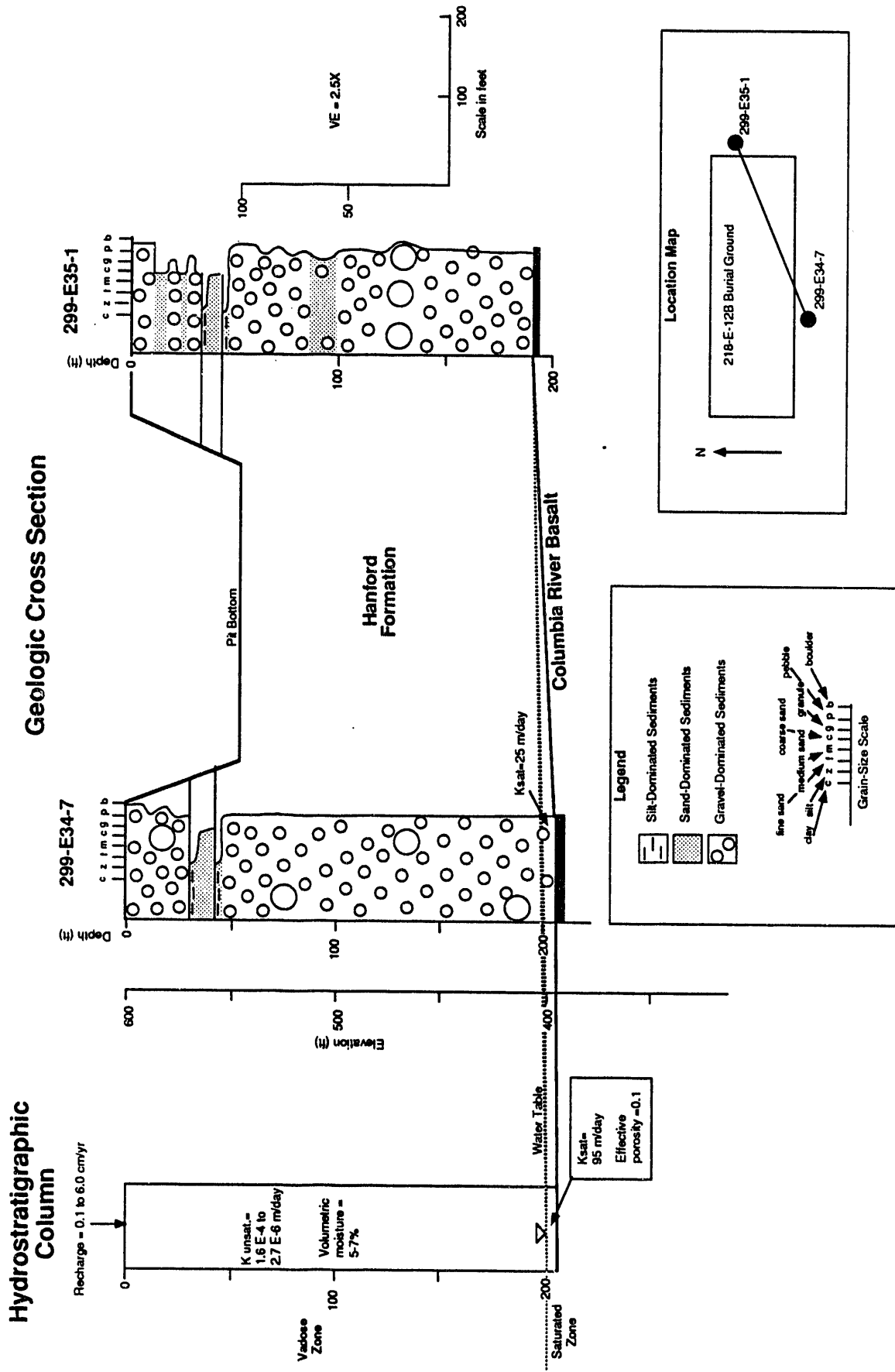


**FIGURE 2.2.** Hydrogeologic Cross Section Beneath the 218-E-12B Burial Ground

correlated to those in adjacent boreholes, partially as a result of the complex history of flooding (Last et al. 1989).

## 2.2 PHYSICAL PROPERTIES OF THE HANFORD FORMATION

Representative data for physical properties of the Hanford formation components are currently limited. Some limitations of physical property data include 1) a bias in favor of the finer-grained sediments (e.g., sand, silt, and clay) because representative samples of coarse-grained sediments are difficult to collect and measure and 2) physical properties that may be significantly altered during sampling (e.g., density increases and hydraulic conductivity decreases due to compaction during coring). For these reasons, *in situ*, field-tested measurements of physical properties are believed to be more representative than those obtained in the laboratory, although in practice they are difficult to obtain. Additionally, samples collected from outcrops are more likely to reflect *in situ* conditions than are borehole samples. The geologic characteristics of the Hanford formation beneath the burial site were determined from previous studies of these soils, as well as from samples taken for this study from the burial pit faces and nearby boreholes. Where good field data were available in the literature, they were used for this assessment. In the absence of such information, the study employed data from laboratory analyses of collected samples. The physical and hydraulic properties of Hanford sediments are summarized in Table 2.1.

The physical properties of the Hanford formation vary depending on sediment type and depth below ground surface. Sediments at greater depth have lower hydraulic conductivities and porosities, and higher densities because of diagenetic effects such as compaction and recrystallization. Gravel-dominated sediments tend to have higher saturated hydraulic conductivities and densities (1.8 to 2.0 g/cm<sup>3</sup>), as well as lower total porosity (0.2 to 0.4) and moisture (1 to 5 wt%) compared with fine-grained sediments. The gravel-dominated sediments are usually more poorly sorted and display characteristic large-scale foreset bedding, with dips up to 30 degrees from horizontal. Maximum clast size ranges from pebbles to boulders greater than 1 m in diameter. Gravel-dominated sediments often grade upward into sand- and silt-dominated sediments. The sand-dominated sediments are intermediate in most

**TABLE 2.1. Physical and Hydraulic Properties of Hanford Formation Sediments in the Vicinity of the 218-E-12B Burial Ground**

PROPERTY	VADOSE ZONE SEDIMENTS				SATURATED ZONE SEDIMENTS
	Silt-Dominated	Sand-Dominated	Gravel-Dominated	Undifferentiated	
Saturated Hydraulic Conductivity (m/day)					
• Laboratory Tested	0.15-4.05 (1)	1.0-9.4 (1)	3-95 (2)	9-25 (2) 0.3-30 (1)	Not Available
• Field Tested	Not Available	Not Available	Not Available	Not Available	25 (3) 450-27,500 (4) 600-3050 (5)
Unsaturated Hydraulic Conductivity (m/day)	Not Available	Not Available	Not Available	Not Applicable	Not Applicable
Density (g/cm <sup>3</sup> )	1.4-1.6 (1)	1.3-1.7 (1)	1.8-2.0 (1)	Not Applicable	1.8-2.0 (1)
Total Porosity	0.3-0.5 (1)	0.3-0.5 (1)	0.2-0.4 (1)	Not Applicable	0.2-0.4 (1)
Effective Porosity	Not Applicable	Not Applicable	Not Applicable	Not Applicable	0.1 (6)
Moisture (wt%)	5-30 (1)	1-5 (1)	1-5 (1)	Not Applicable	Not Available
Moisture (vol.%) (saturated)	Not Applicable	Not Applicable	Not Applicable	Not Applicable	20-30
Percent Gravel	0	0-60	60-100	Not Applicable	(7)
Percent Sand	0-50	50-100	0-60	Not Applicable	(7)
Percent Silt	50-100	0-50	0-20	Not Applicable	(7)
Percent Clay	0-10	0-5	0-5	Not Applicable	(7)

Sources: (1) Laboratory results obtained for this project

- (2) Bjornstad (1990)
- (3) Borghese et al. (1990)
- (4) Last et al. (1989)
- (5) Graham et al. (1981)
- (6) Bierschenk (1959)
- (7) Values used are assumed to be the same as those for gravel-dominated sediments in the vadose zone.

properties between gravel-dominated and silt-dominated sediments (Table 2.1), and are better sorted than the gravel-dominated sediments. Structurally, the sand-dominated sediments display planar, subhorizontal laminations ranging from millimeters (mm) to centimeters (cm) in thickness.

Silt-dominated sediments (predominantly silt- to fine sand-sized particles) have relatively low saturated hydraulic conductivities (0.15 to 4.05 m/day) and densities (1.4 to 1.6 g/cm<sup>3</sup>). Silt-dominated sediments compose a relatively small proportion of the Hanford formation within the 218-E-12B Burial Ground. However, they are significant because they tend to concentrate and control vadose-zone transport of moisture as a result of their higher moisture retention capacity (up to 30 wt%). Two thin (a few feet or less) silt-dominated beds are present in the upper 15 m (50 ft) of the exposed faces at the 218-E-12B Burial Ground (Figure 2.2). Additional silt beds may be present at depths below 15 m, but they are difficult to identify from drilling logs because of their limited thickness and higher densities that result from compaction at these depths.

### 2.3 HYDROLOGY

Groundwater in the vicinity of the 218-E-12B Burial Ground occurs under both unconfined and confined conditions. The focus of this report, however, is on the vadose zone and unconfined aquifer (Figure 2.2). The unconfined aquifer, which is generally  $\leq 3$  m thick in the vicinity of the burial ground, occurs within the Hanford formation. Point measurements of the saturated thickness of the unconfined aquifer beneath the 218-E-12B Burial Ground range from  $\leq 0.6$  to 1.3 m. However, the unconfined aquifer is thicker both north and south of the burial ground. Columbia River basalt forms a relatively impermeable confining layer beneath the Hanford formation. Aquifer tests within gravel-dominated sediments of the Hanford formation indicated that saturated hydraulic conductivities in these Hanford soils ranged from 25 to 27,500 m/day (Table 2.1). The highest hydraulic conductivity values measured at the Hanford Site were associated with matrix-depleted bouldery gravels, which are generally not present beneath the 218-E-12B Burial Ground. In contrast, the saturated hydraulic conductivity of basalt underlying the

unconfined aquifer is less than 1 m/day in the horizontal direction and  $3 \times 10^{-5}$  m/day in the vertical direction (Lum et al. 1990).

To the south of the 200-West and 200-East Areas, the regional groundwater flow is currently from west to east. The groundwater flow direction in this area is controlled primarily by recharge from the Cold Creek and Dry Creek drainages (located to the southwest of the Site), an artificial recharge mound associated with B Pond, and the Columbia River. The B Pond consists of a series of unlined, interconnected waste water disposal ponds that receive effluent from the 200-East Area. Discharges to B Pond will be discontinued as activities at the Hanford Site shift to emphasize cleanup. Thus, the present conditions reflecting B Pond operation are not expected to persist. Based on the December 1987 water table shown in Figure 2.3, groundwater in the vicinity of the 218-E-12B Burial Ground is moving from B Pond toward the west, turning north through the gap between Gable Butte and Gable Mountain. Although this general flow pattern would be expected to persist over the near future, the exact level of the water table is subject to short-term fluctuations caused by seasonal variations in precipitation and changes in site operations (Woodruff and Hanf 1991).

For this assessment, two cases of regional groundwater flow in the absence of B-Pond recharge have been simulated -- one showing present climate conditions (0.5 cm/yr recharge) and another illustrating potentially more humid climate conditions (5 cm/yr recharge). Water table contours for these two cases are shown in Figures 2.4 and 2.5. A conceptual model describing the unconfined aquifer beneath the 200-East Area under these conditions is discussed in a subsequent section of this document.

December 1987

Water-Table Contours  
in Feet Above Mean  
Sea Level

— 5-ft Contour

→ Flow Path

0 1 Mile

0 1 Kilometer

Estimated Basalt  
Above Water  
Table

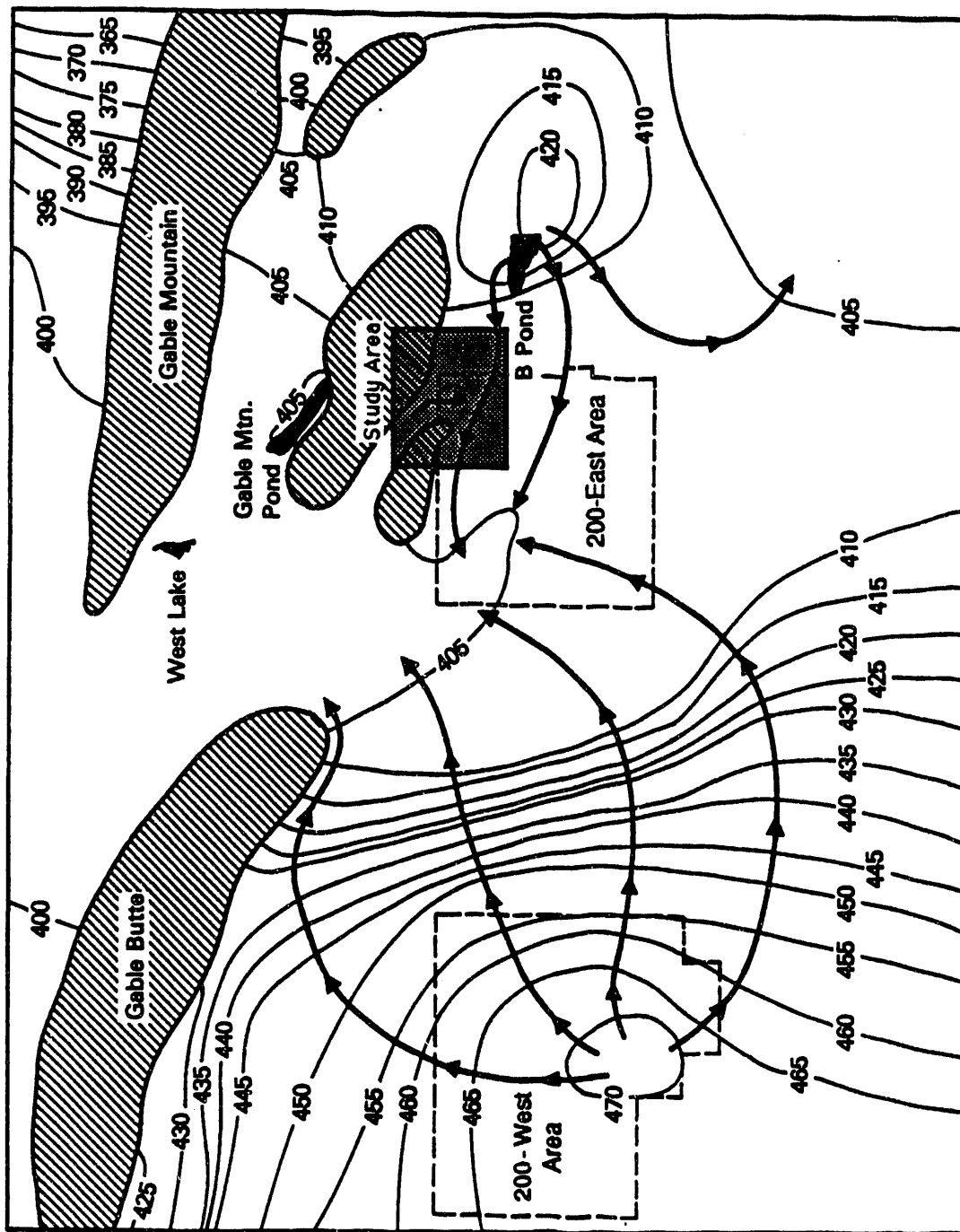
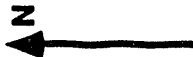
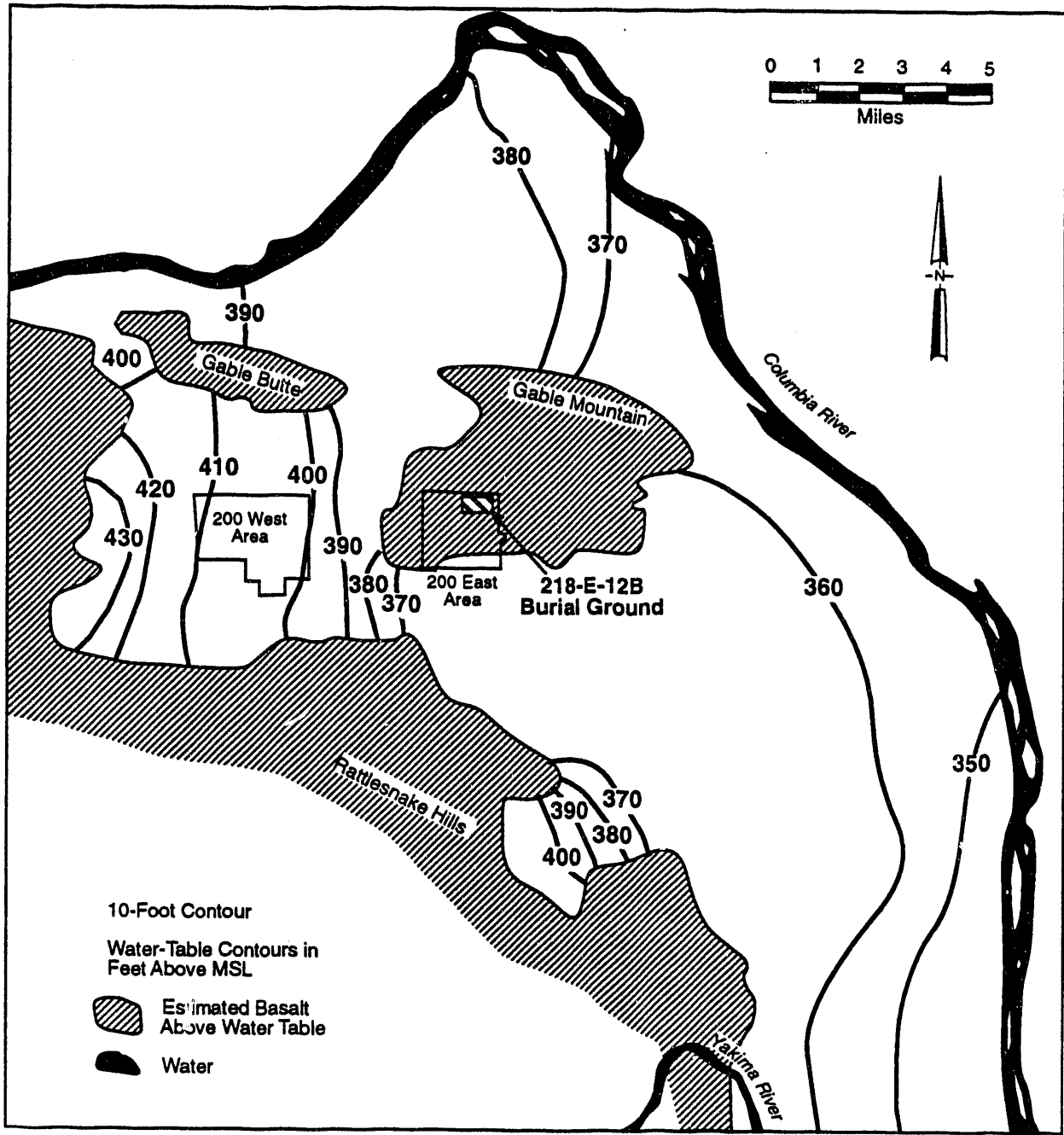
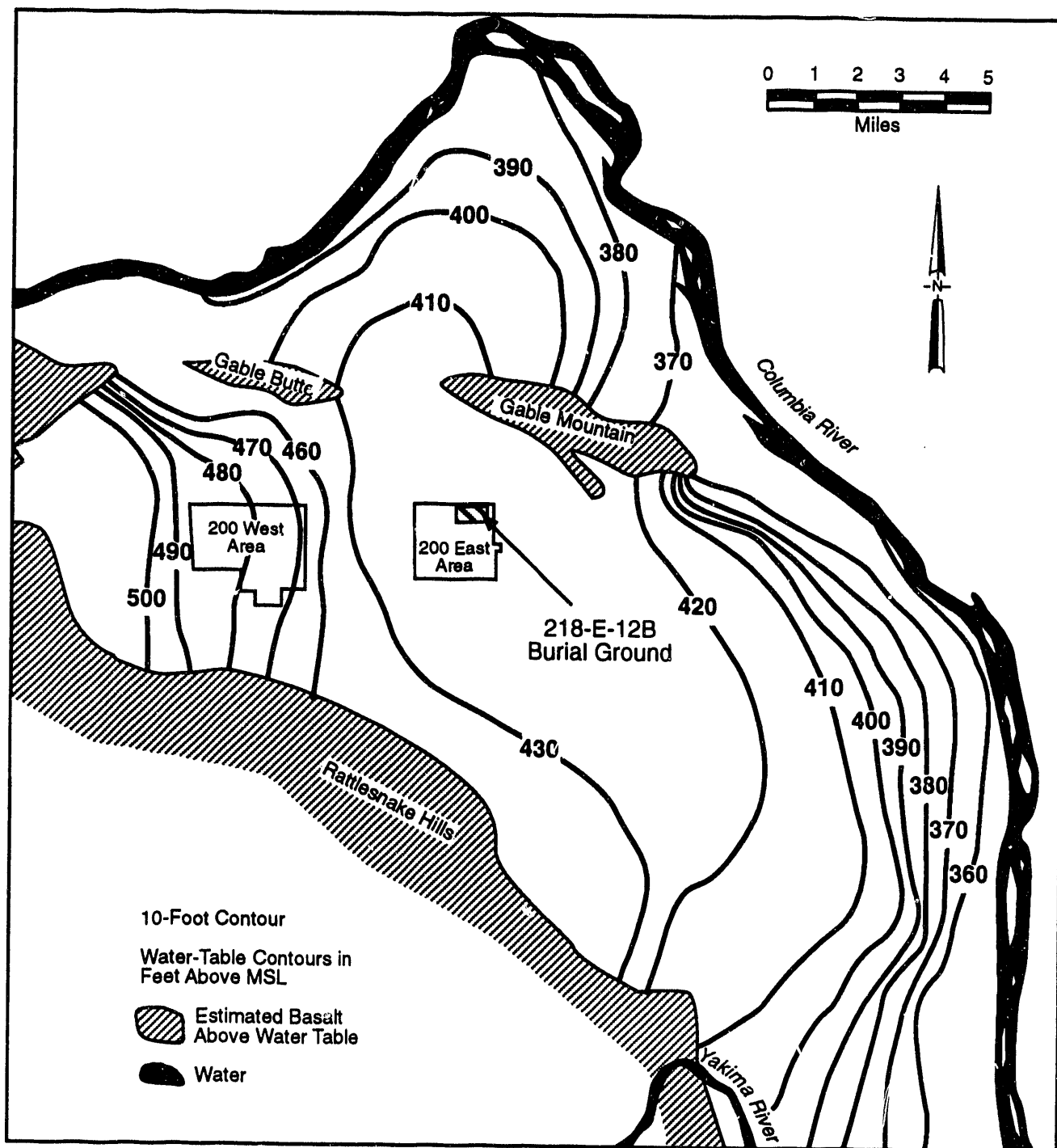


FIGURE 2.3. Presumed Groundwater Gradients and Flow Directions in the Unconfined Aquifer Beneath the Hanford Site 200 Areas



**FIGURE 2.4.** Water Table Contours for the Steady-State 0.5 cm/yr Recharge Case (Graph scales in feet. Contour lines in feet above mean sea level.)



**FIGURE 2.5.** Water Table Contours for the Steady-State 5.0 cm/yr Recharge Case (Graph scales in feet. Contour lines in feet above mean sea level.)

### 3.0 GEOCHEMISTRY OF LEAD IN SOIL/GROUNDWATER SYSTEMS AT THE HANFORD SITE

This portion of the study investigated the solubility and adsorption characteristics of lead in Hanford sediments that exist at the burial site. Possible competitive effects of other materials in the waste components on soil adsorption of lead were also investigated as part of the study. This was considered because the presence of other metals could reduce adsorption of lead in the soil column and thereby accelerate its transport to downgradient groundwater locations. Iron, chromium, and nickel are also significant constituents in the waste, and of the three only nickel is sufficiently soluble in a chemical form that could compete with lead for soil adsorption sites. Therefore, this investigation included experiments to determine whether nickel might influence adsorption of lead in Hanford sediments. Estimates of the release of lead and nickel from the waste components, and their removal by geochemical processes as they move with soil water through the subsurface, depend upon corrosion rates in the waste components, chemical form of the released metals, their mobility, and their probable interactions with aqueous geochemistry and sediment mineralogy beneath the site.

As part of this task, a literature search and geochemical modeling were performed to determine solubility constraints for lead and nickel in Hanford groundwater and soil pore water. An empirical solubility experiment was conducted to verify the accuracy of the MINTEQA solubility calculations. Batch adsorption studies were conducted to determine the distribution coefficients ( $R_d$ ) for lead on Hanford sediments, as well as to investigate potential competitive effects of nickel on lead adsorption. Flow-through column experiments were performed to confirm the results of the batch experiments.

#### 3.1 METHODS FOR DETERMINING LEAD AND NICKEL SOLUBILITY

Metallic lead and nickel will be present in the burial ground as solid lead metal and nickel alloy steel. Groundwater transport predictions require knowledge of the rate at which solid forms of the metals leach into solution as well as their soil adsorption properties as discussed in the following sections. For this analysis, leaching of lead and nickel from the metal waste components was treated as a thermodynamic solubility process. That is, it was

assumed that recharge water percolating through the burial ground contacts the buried wastes and instantaneously oxidizes and dissolves enough metal to achieve equilibrium with the lead and nickel compounds that would be thermodynamically stable under these conditions. This approach ignored any kinetic and mass transfer hindrances to dissolution that are likely to lower the concentration of lead in leachate from the buried wastes, and, therefore, provides a theoretical upper bound for the flux of lead into groundwater.

The solubility of lead in Hanford groundwater was estimated using two methodologies. The first method utilized solubility calculations with the MINTEQ geochemical equilibrium code (Felmy et al. 1984). The composition of groundwater used in these calculations was determined for water taken from well 6-S3-25 and is listed in Table 3.1. This well is located in the general vicinity of the 200 Area, but is sufficiently remote that it is relatively uncontaminated by liquid discharges from operating facilities. Based on the well water analysis shown in Table 3.1 and assuming equilibrium with the solid phases of plausible lead and nickel compounds, the MINTEQ code was used to calculate equilibrium solution concentrations for these compounds.

In the second method, lead solubility was determined empirically by equilibrating lead metal with Hanford groundwater. After the equilibration period, the solution was filtered with an Amicon CF 25 Centriflo membrane filter cone with a nominal 18-angstrom pore size. The lead in these solutions was analyzed by Inductively Coupled Plasma-Mass Spectroscopy (ICP-MS). Prior to use the filter was treated by soaking overnight in deionized water and then passing 5 mL of Hanford groundwater through the filter.

### 3.2 DESCRIPTION OF ADSORPTION EXPERIMENTS

The following sections describe procedures used to prepare soil samples for laboratory analyses and to conduct adsorption studies. Batch tests were performed to provide data for transport modeling, and a flow-through column test was conducted to confirm the results of batch tests.

**TABLE 3.1. Chemical Composition of Hanford Groundwater<sup>(a)</sup> (Well 6-S3-25) That Was Input to MINTEQ Computer Code for Determination of Solubility for Lead and Nickel Compounds**

<u>Chemistry</u>	<u>Sample Used (4/90)</u>	<u>Range in Composition (1985-1990)</u>
pH	8.14	7.82 - 8.47
Eh(mv)	309	283 - 385
Cations (meq/L) <sup>(b)</sup>	5.29	4.9 - 5.4
Anions (meq/L)	4.60	4.6 - 6.1

**Constituents:**

Al	<0.03	<0.03 - 0.064
B	0.1	0.02 - 0.10
Ba	0.08	0.04 - 0.08
Ca	48.8	48.8 - 58.8
Cd	<0.004	<0.004
Cr	<0.020	<0.02 - 0.034
Cu	<0.004	<0.004
Fe	<0.005	<0.005 - 0.008
K	9.9	4.9 - 9.9
Li	<0.004	<0.004
Mg	14.6	13.2 - 14.6
Mn	<0.002	<0.002 - 0.13
Na	32.1	23.8 - 32.1
P	<0.1	<0.1
Pb	<0.06	<0.06
Si	16.4	14.6 - 16.4
Sr	0.25	0.23 - 0.25
Zn	<0.02	<0.02 - 0.08
F <sup>-</sup>	0.5	<0.5 - 0.7
Cl <sup>-</sup>	27	21 - 27
NO <sub>2</sub> <sup>-</sup>	<0.3	<0.3
NO <sub>3</sub> <sup>-</sup>	<0.5	<0.5
PO <sub>4</sub> <sup>3-</sup>	<0.4	<3
SO <sub>4</sub> <sup>2-</sup>	75	63 - 92
T-Alk (as CO <sub>3</sub> <sup>2-</sup> )	67.5	67.5 - 92.4
TOC	1	0.3 - 1.7

(a) From: Serne, R. J., V. L. LeGore, C. W. Lindenmeier, J. A. Cambell, and J. L. Conca. 1991. Progress on Task D Performance Assessment Support in the Solid Waste Technology Support Project. Pacific Northwest Laboratory, Richland, Washington.

(b) One equivalent (eq) equals the gram-atomic mass of a given cation divided by its ionic charge.

### 3.2.1 Preparation and Analysis of Hanford Sediment Samples

Approximately 45 kg of sediment representative of the most common material in the pit wall strata were collected near the base of the burial trench. This material weighed 43.4 kg after air drying, and 29.2 kg of finer soil remained after screening out the coarser (>2 mm) material. The 14.2 kg of coarse gravel was discarded and the "fine" material was used in all further characterization and laboratory studies to determine the geochemical fate of lead. The "fines" included sand, silt, and clay, which were thoroughly mixed prior to characterization and laboratory studies. The silt and clay size fractions of the "fines" were characterized using X-ray diffraction (XRD) to determine mineralogy. Analyses for calcium carbonate content, total cation exchange capacity, organic carbon, and particle size have also been completed.

### 3.2.2 Batch Adsorption Tests

The primary metal of interest in this study was lead. The distribution coefficients ( $R_d$ ) for lead were measured both in the absence and presence of nickel using batch adsorption tests, and the batch  $R_d$  values were corroborated using flow-through column tests. The experimental details for performing both batch and column adsorption tests are described in Relyea et al. (1980), Relyea (1982), and Serne and Relyea (1983); a theoretical discussion of adsorption mechanisms appears in Appendix A. The specific experiments performed for this study included batch adsorption tests using fines from samples collected at the burial trench, and a representative Hanford groundwater (from well 6-S3-25) spiked with lead at initial concentrations ranging from  $3.0 \times 10^{-8}$  M (6.2  $\mu\text{g/L}$ ) to  $1.0 \times 10^{-6}$  M (207  $\mu\text{g/L}$ ). The potential competitive effects of nickel on adsorption of lead were studied by varying the lead concentrations in the presence of an initial nickel concentration of  $5.0 \times 10^{-5}$  M (2.9 mg/L). The solution-to-solid ratio used in the batch tests was approximately 30 mL:1 g, with contact times of 7, 10, or 30 days. Solution was separated from soil using both centrifugation and filtration through 0.22- $\mu\text{m}$  membranes.

The methodologies described above were used to determine the bulk of the  $R_d$  values in this study. In order to obtain  $R_d$  data at very high lead concentrations in the sediment, another experimental methodology was

developed. In this case, a very large solution-to-solid ratio was used so that the sediment would adsorb a large amount of lead but the concentration of lead in solution would remain relatively high. To accomplish this, one gram of sediment was placed in each of two chromatography columns, and ten liters of a groundwater solution containing 207  $\mu\text{g/L}$  lead with radioactive tracer was continuously recirculated through the columns and back to the solution reservoirs at a flow rate of approximately 3 mL/minute. After one week, the tracer radioactivity in the equilibrium solution and sediment from each experiment was counted directly.

The lead  $R_d$  values were determined using two different analytical techniques. Some batch tests contained  $^{210}\text{Pb}$  tracer that was measured using gamma ray spectroscopy, whereas other tests contained only stable lead that was measured in solution using ICP-MS. When only solution concentrations could be measured (stable lead experiments), concentrations in the initial solution (influent or pre-contact solution) and the final solution (effluent separated at the end of the batch contact) were measured. The mass difference between the influent and effluent was assumed to equal the amount adsorbed onto the sediment. The  $R_d$  value was then calculated using the following equation:

$$R_d = \frac{(C_{\text{inf}} - C_{\text{eff}})}{C_{\text{eff}}} \frac{V}{W} = \frac{C_{\text{soil}}}{C_{\text{solution}}} \frac{V}{W} \quad (3.1)$$

- where
- $C_{\text{inf}}$  = lead concentration or tracer activity in influent solution (g/mL or counts/mL)
  - $C_{\text{eff}}$  = lead concentration or tracer activity in effluent solution (g/mL or counts/mL)
  - $C_{\text{soil}}$  = lead concentration or tracer activity in the soil (g solute/g soil or counts tracer/g soil)
  - $C_{\text{solution}}$  = lead concentration or tracer activity in solution (g/mL or counts/mL)
  - $V$  = volume of solution used (mL)
  - $W$  = weight of soil used (g).

Equation (3.1) was used to calculate  $R_d$  values for lead in the experiments where only stable lead was present.

In the experiments that contained  $^{210}\text{Pb}$  plus stable lead, the sediment containing adsorbed  $^{210}\text{Pb}$  was also counted to permit determination of  $R_d$  values directly using Equation (3.2):

$$R_d = \frac{S}{C} \quad (3.2)$$

where  $S$  = activity of tracer per gram of soil

$C$  = activity of tracer per mL of effluent solution,

as well as indirectly with Equation (3.1). In general, the  $R_d$  values calculated using Equation (3.2) were considered more accurate for these tests because they are not affected by adsorption of tracer onto the container walls.

### 3.2.3 Column Adsorption Tests

A flow-through column experiment was performed to corroborate the  $R_d$  values calculated for lead using the batch adsorption experiments. In order to obtain data in a timely manner, the flow-through column test was conducted at a relatively rapid flow rate (approximately 10 pore volumes/day). The residence time for groundwater in the column test was therefore only 2.4 hours, which is extremely short compared with the predicted residence times of recharge water in the vadose zone sediments at Hanford (50 to 2150 yr, see Section 4.2). Conditions in the flow-through column test thus represent extremes that are likely to over-predict lead mobility based on adsorption kinetics and colloidal transport potential. The extremely short residence time in the laboratory column test could potentially prevent some soil adsorption that would normally occur at lower flow rates. The kinetic energy imparted to the system as a result of the higher flow rate might also promote colloidal transport. Therefore, the column test should represent worst-case conditions for lead adsorption, in addition to providing a check on whether other processes not adequately covered by batch adsorption tests (e.g., multiple speciation) are important in this geochemical system.

The column test allowed for direct determination of the retardation factor ( $R_f$ ) from the number of pore volumes of effluent required to reach a breakthrough ratio,  $C_{\text{eff}}/C_{\text{inf}}$ , of 50%. A 24-mL sediment column was contacted

with Hanford groundwater that had been spiked with stable lead at a concentration of approximately 250  $\mu\text{g/L}$  (near the predicted maximum solubility of lead). Effluent solutions were analyzed using the same methods used in the batch experiments. From the observed breakthrough curve and retardation factor, the  $R_d$  values can be calculated using Equation (3.3)

$$R_f = 1 + \rho_s[(1 - \eta)/\eta]R_d \quad (3.3)$$

where:  $R_f$  = the retardation factor  $v_w/v_n$  (velocity of water  $\div$  velocity of solute)

$\rho_s$  = particle density of the soil material (mass/unit volume)

$\eta$  = porosity (dimensionless)

and  $R_d$  = distribution coefficient (mL/g)

because  $R_f$  is measured and  $\rho_s$  and  $\eta$  are obtained during the test set up.

### 3.3 RESULTS AND DISCUSSION

The following sections present results of the characterization of Hanford sediments in the vicinity of the 218-E-12B Burial Ground, the laboratory experiments to determine the solubility of lead and nickel in Hanford groundwater, and the extent of adsorption of lead on these sediments in the presence and absence of nickel.

#### 3.3.1 Sediment Characterization

The sediment characterization data collected are shown in Tables 3.2 through 3.6. Table 3.2 shows the particle size distribution of the "fines" used in all lab tests and the *in situ* sample taken from the field. The particle size distribution was determined by combining dry sieving and a modified pipet method (using a centrifuge) to separate silt from clay. The dry sieving showed that most of the material was between 1 and 2 mm in diameter. Texturally the sediment would be considered a very coarse sand. The particle density of the fines used in laboratory testing was 2.84  $\text{g/cm}^3$ , similar to most Hanford sediments. The saturated paste pH and saturation extract composition are given in Table 3.3. Table 3.4 shows the percent of amorphous hydrous oxide, calcium carbonate, and total organic carbon in the

**TABLE 3.2.** Particle Size Distribution of Hanford Formation Sediments in the Vicinity of the 218-E-12B Burial Ground

<u>Sediment Type/Size</u>	<u>Percent by Weight</u>	
	<u>Fines Used in Adsorption Studies</u>	<u>In Situ Composition of Vadose Zone Sediments</u>
Gravel (>2mm)	0.00	32.7
Sand (<2mm to >63 $\mu$ m)	99.55	67.0
Silt (<63 $\mu$ m to >2 $\mu$ m)	0.39	0.26
Clay (<2 $\mu$ m)	0.06	0.04

**TABLE 3.3.** Saturation Paste pH and Composition of Soil from the 218-E-12B Burial Ground<sup>(a)</sup>

<u>Saturation Paste pH</u>	8.35
<u>Composition</u>	
<u>Constituent</u>	<u>Concentration (<math>\mu</math>g/g dry soil)</u>
PO <sub>4</sub> <sup>3-</sup>	< 0.07
Cl <sup>-</sup>	6.38
NO <sub>3</sub> <sup>-</sup>	0.97
SO <sub>4</sub> <sup>2-</sup>	16.48
Total Alkalinity (as CO <sub>3</sub> <sup>2-</sup> )	14.52
Na <sup>+</sup>	5.26
Mg <sup>2+</sup>	1.97
Ca <sup>2+</sup>	8.10
Sr <sup>2+</sup>	0.04
Si	3.98
Dissolved Organic Carbon	1.66

(a) From: Serne, R. J., V. L. LeGore, C. W. Lindenmeier, J. A. Cambell, and J. L. Conca. 1991. Progress on Task D Performance Assessment Support in the Solid Waste Technology Support Project. Pacific Northwest Laboratory, Richland, Washington.

**TABLE 3.4.** Amorphous Oxide, Calcium Carbonate and Organic Carbon Content of the "Fines" in Soil from the 218-E-12B Burial Ground

<u>Oxide</u>	<u>Percent by Weight</u>
SiO <sub>2</sub>	0.41
Al <sub>2</sub> O <sub>3</sub>	0.26
Fe <sub>2</sub> O <sub>3</sub>	0.41
MnO <sub>2</sub>	0.02
CaCO <sub>3</sub>	0.82
Total Organic Carbon	≤ 0.01

**TABLE 3.5.** Exchangeable Cations and Total Cation Exchange Capacity for Soil from the 218-E-12B Burial Ground

<u>Cation</u>	<u>Concentration (meq/100 g)</u>
Na <sup>+</sup>	0.12 ± 0.02
Ca <sup>2+</sup>	4.15 ± 0.63
Mg <sup>2+</sup>	0.87 ± 0.03
Total Exchangeable Cations	5.14 ± 0.6
Total Cation Exchange Capacity	5.27 ± 1.2

**TABLE 3.6.** Mineral Content of the Clay Size Fraction of the "Fines" Used in Adsorption Experiments

<u>Mineral</u>	<u>Percent by Weight</u>
Illite	13
Talc	Not Detected
Horneblende	1
Kaolinite	3
Chlorite	2
Vermiculite	8
Smectite	38
Quartz	9
Plagioclase	26

finer. Exchangeable cation results are given in Table 3.5, and the mineralogy of the clay fraction of the sediment is shown in Table 3.6.

The exchangeable cation and total cation exchange capacity analyses suggest that coarse sand has an exchange capacity of about 5 meq/100 g, a value typical of Hanford sediments, especially sands. In fact, given the rather coarse texture of the sediments, we would expect values as low as 3 meq/100 g. The clay size fraction contains crystallites of plagioclase feldspar, quartz, and the clays smectite, illite, vermiculite, and kaolinite. Smectite predominates in the layer silicates, as is generally found for Hanford sediments.

### 3.3.2 Solubility of Lead and Nickel

According to MINTEQ calculations, the solubility of  $Pb^{2+}$  in Hanford groundwater was estimated to be  $1.39 \times 10^{-6}$  M (287  $\mu\text{g/L}$ ) in equilibrium with cerussite ( $PbCO_3$ ). The solubility of lead was determined empirically by allowing lead wool to equilibrate with Hanford groundwater for three months. The unfiltered equilibrated solution had a lead concentration of 482  $\mu\text{g/L}$ . The lead concentration in the first 5 mL of solution passing through the 18-angstrom filter was 383  $\mu\text{g/L}$ . The lead concentration in the second 5 mL of solution passing through the filter was 236  $\mu\text{g/L}$ . It was assumed that 236  $\mu\text{g/L}$  was most representative of the actual equilibrium concentration of lead in this solution, and that the higher values originally observed were biased by suspended colloidal particles. Analysis of the whitish precipitate by XRD indicated that it was hydrocerussite rather than cerussite. This was later confirmed by x-ray absorption spectroscopy (XAS).

These results indicate that either cerussite is not the most stable phase in equilibrium with Hanford groundwater, as indicated by the MINTEQ runs, or that the formation of cerussite is kinetically inhibited. The results also suggest that the solubility of hydrocerussite in the test system is much lower than that indicated by the MINTEQ calculations, which predicted a solubility of 510  $\mu\text{g/L}$  in Hanford groundwater. Because of the difficulties in determining thermodynamic solubility products for sparingly soluble solids in geological systems, it is not uncommon for values measured in a particular system to differ from published data. In this case, the difference between

the observed and predicted solubility limits was about a factor of 2, which is relatively good agreement.

MINTEQ calculations indicated that the solubility of nickel should be controlled by  $\text{Ni}(\text{OH})_2$ , and the solubility of  $\text{Ni}^{2+}$  was estimated to be  $2.8 \times 10^{-4}$  M (16.6 mg/L).

### 3.3.3 Batch Adsorption Studies

The first suite of experiments was conducted for a 7- to 10-day equilibration period. Figure 3.1 illustrates the 7- to 10-day  $R_d$  values for lead determined in the radioactive tracer experiments as a function of the final equilibrated lead concentration in solution, both in the presence and absence of an initial nickel concentration of  $5 \times 10^{-5}$  M. This value was chosen to approximate the solubility limit for nickel in Hanford groundwater, allowing a margin of safety to prevent possible precipitation of nickel compounds in the test system. The values for  $R_d$  ranged from 13,000 to 79,000 and the  $R_d$  increased as the concentration of lead in the equilibrated solution decreased. This trend was consistent with expectations, because the relative adsorption of lead should decrease as more adsorption sites on the soil are occupied. The effect is also illustrated in Figure 3.2, where lead adsorption data are plotted as an adsorption isotherm for the radiotracer experiments. When the final concentrations of lead in solution are plotted against those in soil, the concentration of lead in the soil increases in a linear fashion with the concentration in solution (i.e., total adsorption increases). As can be seen from both Figures 3.1 and 3.2, the effect of nickel on lead adsorption was negligible compared with experimental variation in the data.

The 30-day batch  $R_d$  results are shown in Figure 3.3 and are compared with the 7- to 10-day results. Except for two outliers, the 30-day  $R_d$  values appear to be slightly higher, but generally comparable to those obtained in the 7- to 10-day studies. Because infiltration rates in Hanford sediments are extremely low, the 7- to 10-day  $R_d$  values should be conservative estimates of the true values.

Figure 3.4 portrays  $R_d$  results obtained using the non-radioactive lead method, as measured by ICP-MS.  $R_d$  values calculated from these results were substantially lower than those estimated in the radioactive tracer

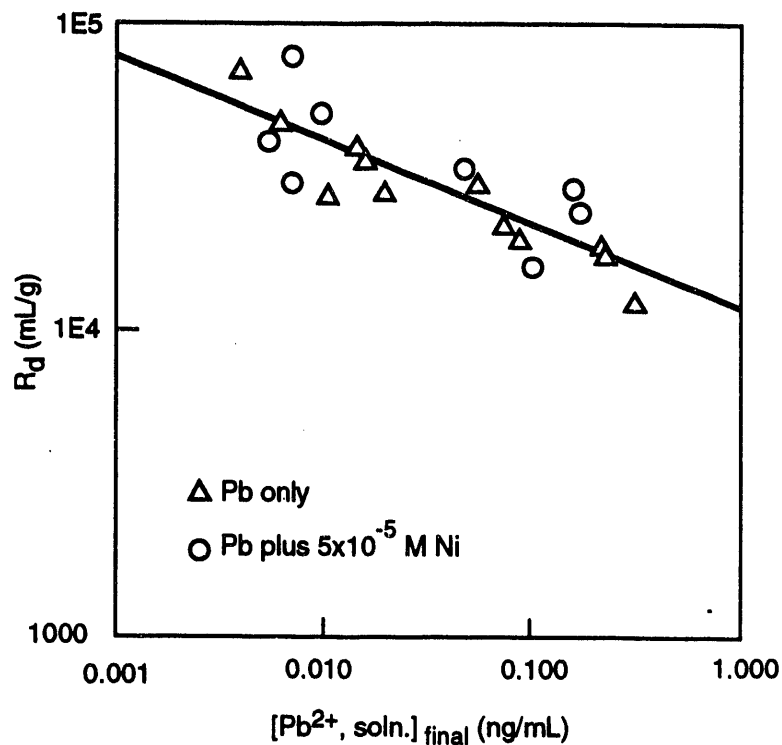


**FIGURE 3.1.** Distribution Coefficients ( $R_d$ ) for Lead from Radiotracer Experiments, 7- to 10-Day Equilibration Period

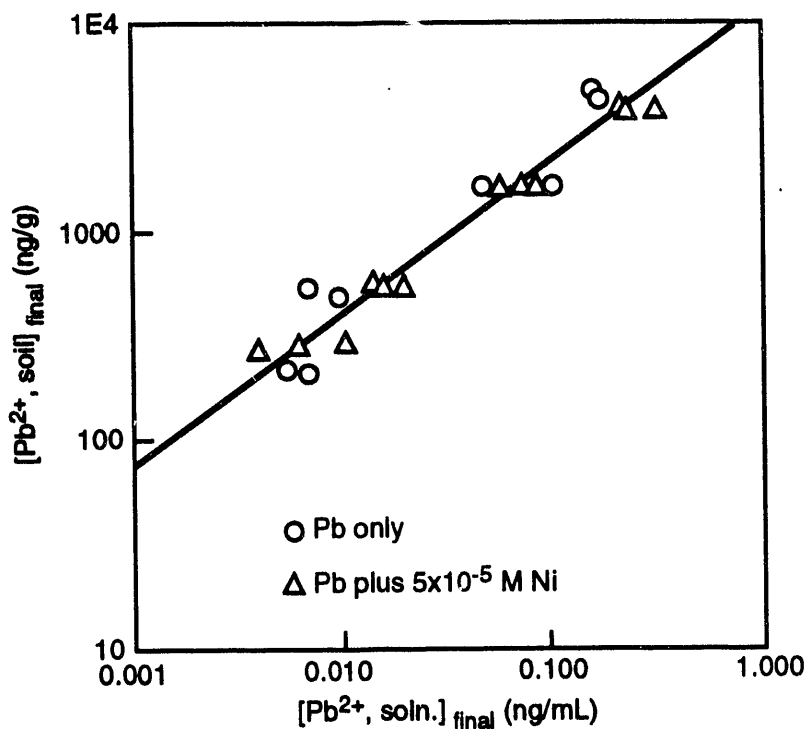


**FIGURE 3.2.** Lead Adsorption Isotherm from Radiotracer Experiments, 7- to 10-Day Equilibration Period

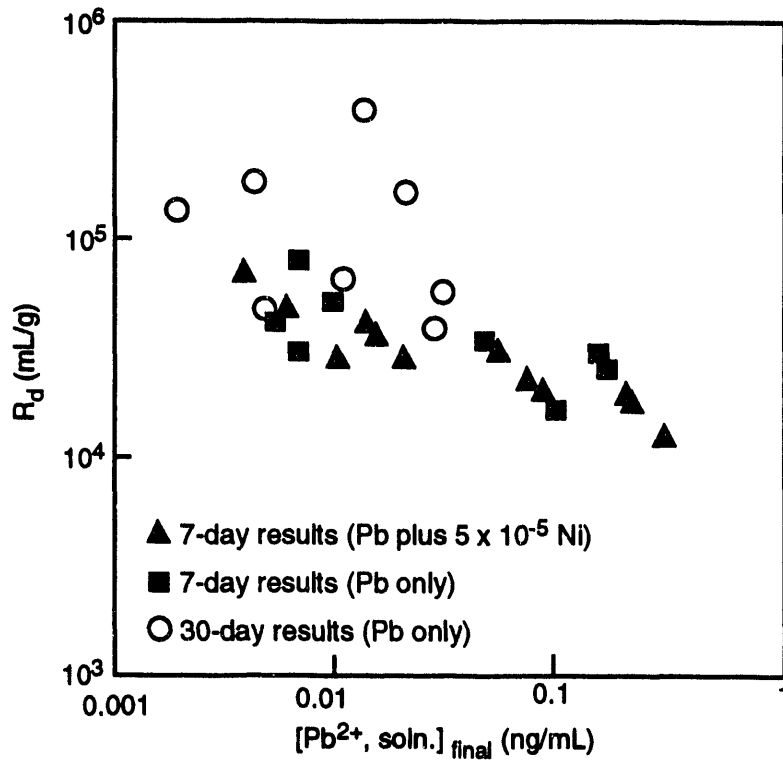


**FIGURE 3.3.** Distribution Coefficients ( $R_d$ ) for Lead from Radiotracer Experiments, Comparison of Values for 7- to 30-day Tests

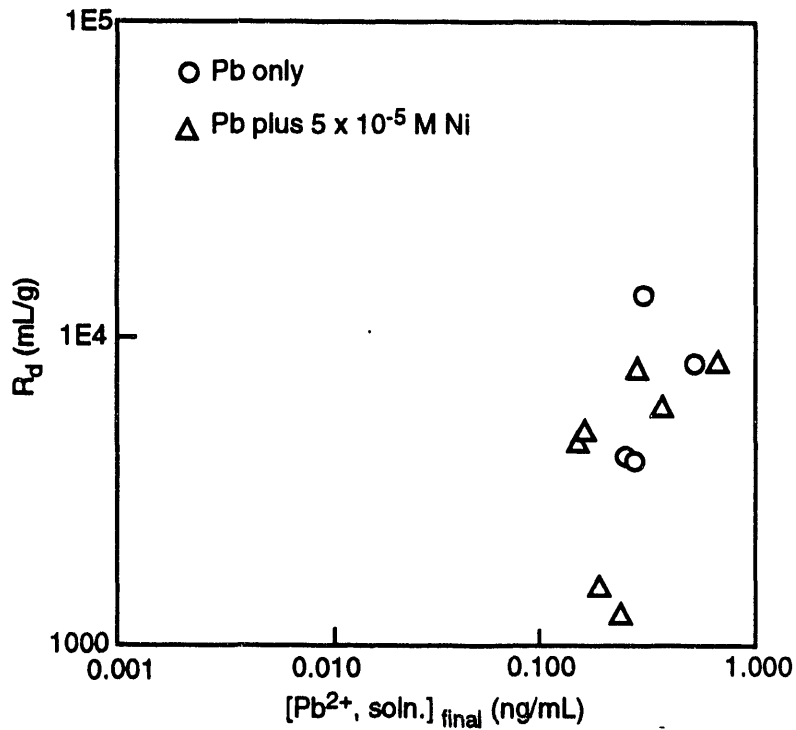


**FIGURE 3.4.** Distribution Coefficients ( $R_d$ ) for Lead from Experiments Without Radioactive Tracer

experiments. This effect is better illustrated in Figure 3.5, which shows the equilibrium isotherm for lead determined by ICP-MS after a 7-day equilibration period. Note that the lead concentrations in sediment were very similar to those shown in Figure 3.2 for the radiotracer experiments; however, the lead concentrations in solution were generally much higher for the ICP-MS results than those determined using the radiotracer technique. These anomalous results appeared to be related to a systematic error in the ICP-MS method for analysis of solutions where lead concentrations approach the detection limit. For example, the lowest lead concentration reported in Figure 3.5 was  $0.15 \mu\text{g/L}$ . In comparison, lead concentrations averaging  $0.21 \mu\text{g/L}$  were reported for five solutions containing various amounts of nickel (measured in a separate nickel-only adsorption study), but to which no lead had been added. As a result, it appears that reported lead concentrations in the  $0.2 \mu\text{g/L}$  range and lower should be considered suspect.

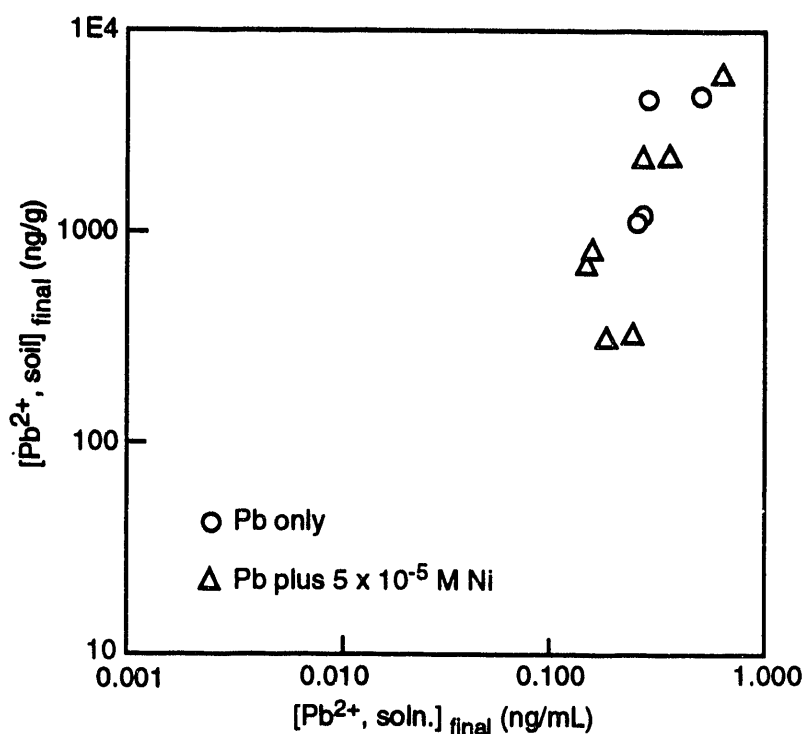


**FIGURE 3.5.** Lead Adsorption Isotherm from Experiments Without Radioactive Tracer

The ICP-MS detection limit for lead in the analytical laboratory was theoretically about 0.05  $\mu\text{g/L}$  for relatively pure solutions. However, the detection limit in environmental samples would be substantially higher because of the presence of other constituents that could potentially interfere with the analysis. Under the conditions of these experiments, the concentrations of lead in the equilibrated solutions are reported to be near or below 0.2  $\mu\text{g/L}$  (as shown in Figure 3.1). Because gamma spectroscopy analysis of  $^{210}\text{Pb}$  allows for accurate estimates of lead concentration at extremely low levels, we consider the lead  $R_d$  values determined by the radiotracer technique to be much more reliable than those determined using the ICP-MS method.

As a result of the strong adsorption of lead onto Hanford sediments, and the fact that the initial lead concentrations were solubility limited, the solution concentration values at equilibrium (illustrated in Figure 3.1) were relatively low (0.005 to 0.3  $\mu\text{g/L}$ ). Based upon the experimental data, the initial lead concentration in the vicinity of the burial site is expected to be limited by the solubility of hydrocerussite  $\text{Pb}_3(\text{CO}_3)(\text{OH})_2$ . Our experimental determination of lead solubility in Hanford groundwater was 236  $\mu\text{g/L}$ . Because  $R_d$  values depend strongly on the equilibrium lead concentration in solution (see Figure 3.1), it would be desirable to obtain the  $R_d$  value at an equilibrium concentration near the solubility limit of lead in Hanford groundwater. For example, if the data in Figures 3.1 or 3.2 are extrapolated to a lead concentration in solution of 236  $\mu\text{g/L}$ , using Equation (3.4),

$$R_d = 1.2 \times 10^4 \cdot C^{-0.274} \quad (3.4)$$

an  $R_d$  value of  $2.7 \times 10^3$  mL/g is estimated. The parameter C in Equation (3.4) is the lead concentration in  $\mu\text{g/L}$  (ppb). In order to get experimentally determined  $R_d$  values at lead concentrations near the solubility limit, two experiments were conducted in which one gram of sediment was equilibrated with 10 liters of a solution containing 207  $\mu\text{g/L}$  lead for approximately 7 days. Figure 3.6 contains the same data as 3.1 with the addition of these two data points. The actual results were  $R_d = 1670$  at 187  $\mu\text{g/L}$  lead and  $R_d = 1190$  at 200  $\mu\text{g/L}$ . These values are about 50% of those predicted from Equation (3.4),

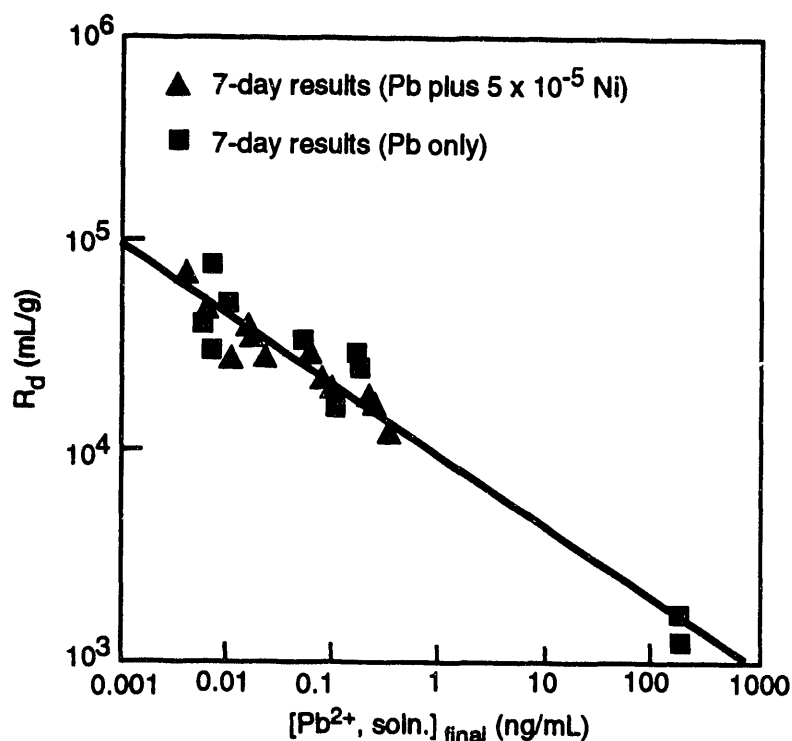


**FIGURE 3.6.** Distribution Coefficients for Lead Experiments with Radioactive Tracer, Including Values Determined Near the Solubility Limit of Lead

which was subsequently revised based on the data shown in Figure 3.6. The new parameters are included in Equation (3.5).

$$R_d = 9550 \cdot C^{-0.335} \quad (3.5)$$

Several batch adsorption experiments were conducted as a function of added calcite. Figure 3.7 illustrates the results. The initial lead concentration in these solutions was 207  $\mu\text{g/L}$  and can be compared with the data in Figure 3.1 having the highest final solution concentrations. The added calcite does appear to cause some increase in the observed  $R_d$  values. The equilibration period does not appear to have a significant effect on the results. It should be noted that the effect of added calcite in these experiments is probably greatly exaggerated relative to the effect of natural calcite in the sediment. This is because the calcite was added as a powder which will have a surface area much greater than that which occurs in natural calcite.

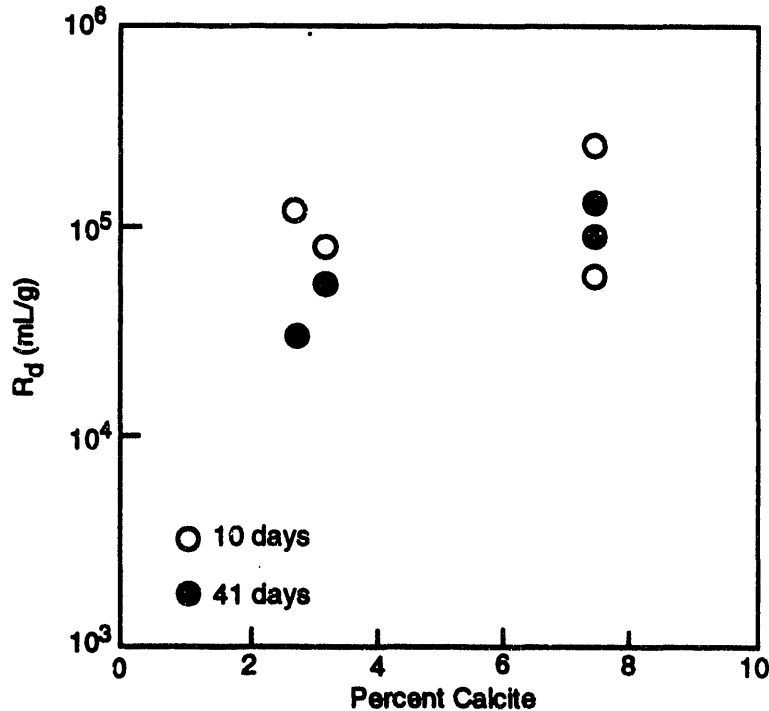


**FIGURE 3.7.** Lead Distribution Coefficient as a Function of Added Calcite

### 3.3.4 Column Adsorption Study

A column adsorption experiment was conducted to confirm the validity of the batch adsorption results in a flow-through system, the results of which are shown in Figure 3.8. The influent concentration of  $Pb^{2+}$  was  $1 \times 10^{-6}$  M ( $207 \mu\text{g/L}$ ), and after 900 pore volumes of this solution had passed through the column, there was no evidence that the lead had broken through. This confirms that adsorption onto soil is effectively removing lead from solution. A retardation factor ( $R_r$ ) appropriate for the conditions used in the column test was calculated using Equation (3.3) to be 8440, based on an  $R_d$  of 1600 mL/g, a particle density of 2.84 g/mL, and a porosity of 0.35. The  $R_d$  value was estimated from Equation (3.5) for a solution concentration of  $207 \mu\text{g/L}$  Pb. This result indicates that 50% breakthrough should not occur until over 8000 pore volumes have passed through the column. Although it was impractical to run the column for this long (800 days at the experimental flow rate), the results after 90 days indicate that no unforeseen mechanisms that could significantly accelerate lead transport are operative.

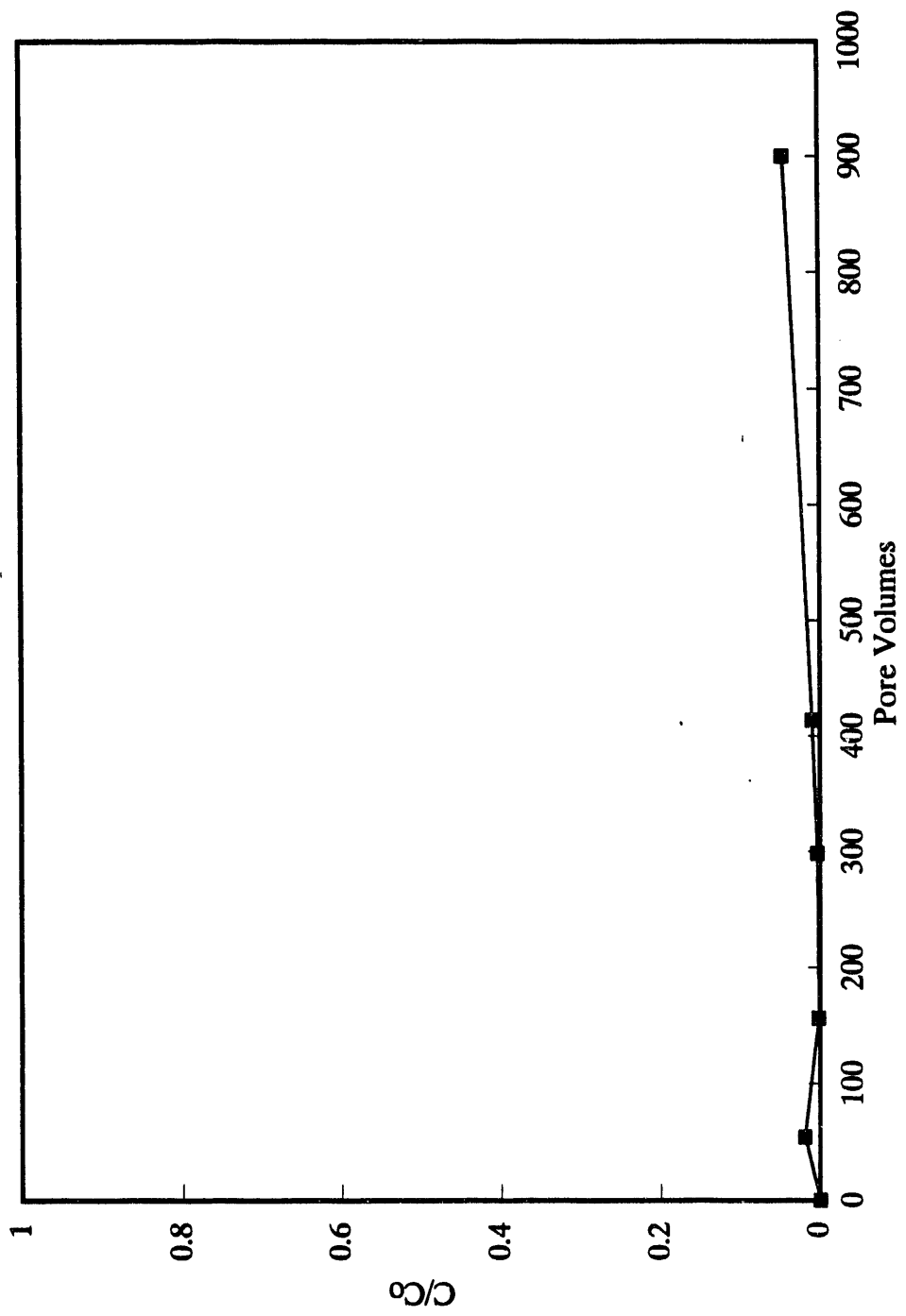


**FIGURE 3.8.** Results of Lead Column Adsorption Experiments

### 3.4 DISCUSSION AND RECOMMENDATIONS FOR TRANSPORT MODELING

Geochemical parameters, as determined in these laboratory studies, were recommended as input for "best estimate" and "conservative" cases in the lead transport model. "Best estimate" values were chosen to represent the expected geochemical behavior of lead at the burial ground, whereas "conservative" values were intended to reflect credible bounding conditions. The solubility limit for lead in Hanford groundwater was determined to be in the range of 236 to 300  $\mu\text{g/L}$  based on the results of laboratory studies and a geochemical model, respectively. The solubility limit for nickel was 16.6 mg/L based on the geochemical model. The "conservative" values for the transport analysis were chosen to be roughly double the "best estimate" values.

The results of batch adsorption studies indicated that  $R_d$  values for lead ranged from  $1.5 \times 10^3$  mL/g near the solubility limit of lead in Hanford groundwater (236  $\mu\text{g/L}$ ) to  $5.6 \times 10^4$  mL/g for equilibrium solution concentrations of lead near 0.005  $\mu\text{g/L}$  (see also Appendix B.7). The  $R_d$  values chosen for modeling were lower than those actually observed in the experiments in order to provide a measure of conservatism in the calculations and to account for the presence of coarser materials in situ beneath the burial ground. The adsorption properties of the coarser gravels could not be measured directly because of physical limitations in the experimental procedures; however, adsorption is expected to be substantially lower in these materials than in the fine-grained soils used for the batch adsorption experiments. Based on the results of solubility and adsorption experiments, the values in Table 3.7 were recommended as "best estimate" and "conservative" estimates for use in groundwater transport modeling.

**TABLE 3.7.** Solubility, Distribution Coefficient ( $R_d$ ), and Retardation Factor ( $R_f$ ) Values Recommended for Use in Transport Modeling

<u>Transport Case</u>	<u>Solubility (mg/L)</u>		<u><math>R_d</math> (mL/g)</u>		<u><math>R_f</math></u>	
	<u>Best Estimate</u>	<u>Conser-vative</u>	<u>Best Estimate</u>	<u>Conser-vative</u>	<u>Best Estimate</u>	<u>Conser-vative</u>
Pb	0.3	0.55	10,000	1200	40,000	4000

#### 4.0 WATER FLOW AND TRANSPORT OF LEAD IN HANFORD SOILS AND GROUNDWATER

In order to estimate rates of groundwater flow and lead transport at the 218-E-12B Burial Ground, a conceptual model was developed for the unconfined aquifer underlying the Hanford Site using available data on geohydrologic properties and geochemistry (as described in previous sections of this report). This section describes a simulation technique used to analyze the migration of lead from waste disposed of at the 218-E-12B Burial Ground and presents the results of the transport analysis.

Metal components in shallow land burials will be subjected to degradation by the natural environment, primarily through chemical weathering and dissolution by infiltrating water. The resulting leachate will drain downward under the influence of gravity until it enters the aquifer, where it will disperse in the groundwater and be transported to the Columbia River. The consequences of lead migration will ultimately depend on the amount of lead in the disposal area, the rate at which it is leached from the buried waste components, and interactions of lead in solution with the soil and water chemistry.

The conceptual model for the burial site was the basis for estimated rates of groundwater movement through the vadose zone and the unconfined aquifer, and for predicted rates of lead migration from the burial ground to downgradient locations and to the Columbia River. The Coupled Fluid, Energy, and Solute Transport (CFEST) code (Gupta et al. 1982; 1987) was used to produce a two-dimensional model of the regional aquifer in order to obtain parameters necessary for the lead transport analysis. The TRANSS code (Simmons et al. 1986) was then employed to simulate mass flow and transport through the vadose zone and the unconfined aquifer using a one-dimensional streamtube approach. This approach is similar to that used in previously published documents for the Hanford Site (DOE 1987; 1989). Simulations were performed for a single component, and for a 4 x 30 array of 120 components on 15-m (50-ft) centers.

Parameters of interest in this investigation, which were incorporated into the simulations, included the following:

- lead inventories for "average-" or "maximum-" sized components (supplied by the client)
- three recharge rates (humid climate, arid climate, and engineered barrier)
- two lead solubilities ("best estimate" and "conservative")
- two lead distribution coefficients ("best estimate" and "conservative")
- three receptor locations (wells at 100 m and 5000 m from the burial site, and the Columbia River).

Several different combinations of these parameters were considered in the analysis to provide estimates for lead transport in the "best estimate" and "conservative" cases.

Lead inventories were assumed to be 227,000 and 455,000 kg for the "average" and "maximum" size individual disposal units, respectively. Groundwater concentrations were estimated for receptors using water from a downgradient well located 100 m or 5000 m from the burial site, and the total annual flux of lead at the Columbia River was also predicted. A groundwater well located 100 m downgradient of the burial ground represents the presumed boundary of the disposal site when institutional control is no longer maintained (DOE 1990a). The groundwater well located 5000 m downgradient represents the location of the family farm scenario that has been used in previous environmental impact statements (EISs) (DOE 1987; 1989).

Specific recharge rates of 6.0, 0.5, and 0.1 cm/yr through the burial ground were modeled for this analysis (Figure 2.2). The 0.5-cm/yr recharge rate, applied to both the burial ground and the Hanford Site, was chosen to represent the present relatively arid climate. The potential effect of a more humid climate on lead transport in the future was modeled using a 6-cm/yr recharge rate for the burial ground and a 5-cm/yr recharge rate for the Hanford regional aquifer model. The 6-cm/yr recharge rate was selected to model the burial ground (in particular, the unsaturated zone) in order to be consistent with previous reports (DOE 1990b; Golder Associates, Inc. 1991) that are based in part on water flow and lead transport at the 218-E-12B Burial Ground. Therefore, using the 6-cm/yr value facilitates comparison of these results with previously reported analyses, and it is not substantially

different from the 5-cm/yr value that was the basis of a previous site-wide analysis characterizing the response of the unconfined aquifer to a more humid climate (DOE 1987; Evans et al. 1988; Jacobson and Freshley 1990). The influence of dryer and wetter climates with respect to the unconfined aquifer at Hanford is described in Section 4.3.2. The 0.1-cm/yr recharge rate represents a conservative estimate of the maximum infiltration that would be expected through a multilayered soil/rock barrier designed to control infiltration over the waste site, as described in a recent EIS for the Hanford Site (DOE 1987).

#### 4.1 ONE-DIMENSIONAL STREAMTUBE APPROACH

A one-dimensional streamtube approach as implemented in the TRANSS code was described by Simmons et al. (1986). A detailed discussion of the streamtube approach and its application was presented in the EIS for disposal of Hanford defense wastes (DOE 1987), and a similar approach was used for this study. This approach assumes transport along a series of streamlines that form a streamtube. Advection was assumed to be the dominant process for lead movement, and transverse dispersion was assumed to be negligible. Advection is defined as contaminant transport in the downgradient direction at the average groundwater velocity, whereas transverse dispersion is transport perpendicular to the direction of the average velocity caused by variations in velocity about the average. Neglecting transverse dispersion in the streamtube resulted in conservation of mass along its entire length from the burial ground to the river.

The streamtube approach of Simmons et al. (1986) is capable of simulating streamtubes that begin in the vadose zone and end at a river, as is expected to be the case for lead migration from the 218-E-12B Burial Ground. Water was assumed to infiltrate vertically through buried waste and to dissolve lead in the components en route to the water table. During transport within the unconfined aquifer, leachate entering the water table from the disposal site was assumed to mix in the upper 2.5 m of the aquifer. The mixing depth of 2.5 m assumed for this analysis was a departure from the 5-m mixing depth used in previous analyses, and it was employed because of the

shallow depth of the unconfined aquifer in the vicinity of the 218-E-12B Burial Ground.

Lead was transported within the streamtube in the unconfined aquifer to downgradient locations and ultimately to the regional aquifer discharge area at the river. Some portion of the dissolved lead may chemically adsorb to the sediments that constitute the geologic units through which the streamtube passes, and a linear adsorption isotherm was incorporated into the model to simulate this process. The following sections describe the conceptualization of the vadose zone and the unconfined aquifer underlying the 218-E-12B Burial Ground, and the rates of water movement through each. The transport of lead to downgradient locations was then estimated for several combinations of key input parameters to the TRANSS computer code.

Two-dimensional and fully three-dimensional groundwater flow and transport codes such as VAM3D and PORFLO-3 will likely be adopted in the near future at the Hanford Site as standard codes for assessing the response of the environment to disposal practices and remediation alternatives. In particular, these and other designated codes, including the CFEST code, will be used for analyses that support the Record of Decision for cleanup actions. The TRANSS code applied for this study is a less sophisticated transport model in terms of its dimensional considerations (it is one-dimensional) and process complexity (it omits transverse dispersion). In general, this less sophisticated code would be expected to overestimate the groundwater concentrations when compared with the results of two- or three-dimensional groundwater flow and transport codes. However, a direct comparison of the results from single- and multi-dimensional models has not been made.

#### 4.2 VADOSE ZONE WATER FLOW

Sedimentary deposits situated between the ground surface and the water table constitute the vadose zone (Figure 2.2). Within these deposits, water only partially fills the available pore space between grains of silt, sand, and gravel, and is generally assumed to drain vertically downward until it enters the unconfined aquifer or until it contacts a low permeability layer of clay or rock. Significant amounts of water that infiltrate the surface soils may be held at the surface and evaporate if the soil cover is sufficiently

fine-grained. Infiltrating water may also be transpired if the surface is covered with vegetation. Any remaining water is assumed to constitute recharge to the underlying aquifer. Fine-grained sediments tend to hold water at the soil surface where the forces for evapotranspiration are greatest; coarse-grained sediments permit the water to drain to a depth where these forces are less effective or nonexistent. The average precipitation at Hanford is currently 16.1 cm/yr. In response to the relatively arid climate interacting with spatially varying soils and temporally varying vegetation, recharge to the unconfined aquifer is variable at the Hanford Site. It ranges from over 10 cm/yr in bare sands and gravels to near zero (non-measurable) amounts in silt-loam soils. As mentioned previously, the local aquifer recharge rate of 0.1 cm/yr (at the burial ground) represents the effect of a multilayered protective barrier of the type being considered for other waste forms (e.g., grouted low-level waste and single-shell tanks) at Hanford. The 0.5-cm/yr local recharge rate represents the present relatively arid climate, whereas the 6-cm/yr local recharge rate (with a regional 5-cm/yr rate) represents a potentially more humid climate that may exist in the future.

Stratigraphic control for the geohydrology in the vicinity of the burial site was obtained from two boreholes (299-E34-7 and 299-W35-1) located immediately adjacent to the burial ground excavation (Figure 2.2). Sediments below the 218-E-12B Burial Ground are composed primarily of gravel-dominated sediments mixed with variable amounts of sand and silt. Gravels are predominantly in the pebble-to-cobble size range, but boulders are occasionally present. The vadose zone is approximately 61 m (200 ft) thick in the vicinity of the 218-E-12B Burial Ground, of which approximately 15 m (50 ft) has been excavated for disposal of the metal components. The thickness of the vadose zone is similar for all simulations because the unconfined aquifer beneath the burial ground is less than 3-m thick in the vicinity of the burial ground, even in the presence of artificial recharge from current site operations (see Section 2.3). The resulting distance from the base of the disposal area to the bottom of the vadose zone is approximately 46 m (150 ft). This analysis did not account for the presence of backfill around the metal components; all water and leachate flow through the 46-m thickness of vadose zone was assumed to begin at the bottom level of the pit. Therefore, the time

required for, and distribution of, water flow through the upper 15 m of the soil profile have not been evaluated as part of this analysis.

The physical properties of sediment samples collected from the faces of the 218-E-12B Burial Ground pit were analyzed in the laboratory; the results are summarized in Table 2.1. Samples could only be analyzed from those portions of the geologic profile without large cobbles or boulders; therefore, analytical data are biased in favor of the finer-grained sediments. Measurements of saturated hydraulic conductivity for these samples (i.e., sand- and silt-dominated) ranged from approximately 0.3 to 30 m/day (1 to 100 ft/day). The soil sample descriptions and saturated hydraulic conductivity data were used to match the significant geologic units in the vadose zone to moisture-retention data measured previously for samples from the Hanford formation in the vicinity of the burial ground (Bjornstad 1990). Because of the larger pebbles, cobbles, and boulders in many horizons, the measured samples were assumed to be representative of the lowest conductivity samples in the geologic section.

Moisture-retention and saturated hydraulic-conductivity data from well 299-E33-30 at the 42.4- to 42.7-m (139- to 140-ft) depth interval were assumed to represent the Hanford formation in the area (Bjornstad 1990). This well is located in the 200-E Area, approximately 2 km west of the 218-E-12B Burial Ground. Samples from this location had the highest measured saturated hydraulic conductivity of any of the samples, approximately 95 m/day. However, it is expected that there are strata within the vadose zone with conductivities above and below this value. The value of 95 m/day is within an order of magnitude of a saturated hydraulic conductivity (25 m/day) obtained from an aquifer test within the saturated zone at well 299-E34-7 (Borghese et al. 1990), immediately adjacent to the burial ground (see Figure 2.2). It is important to note that the vadose zone consists of a sequence of units that contain a range of hydraulic properties. The 299-E33-30 sample was assumed to be representative of the overall profile. The validity of this interpretation is limited by our inability to measure the physical and hydraulic properties of the coarser-grained units, which would be expected to have the highest values. The highest hydraulic conductivity values measured at the Hanford Site, hundreds to thousands of meters per day (Last et al. 1989), are probably

associated with matrix-depleted bouldery gravels, which are generally not present beneath the 218-E-12B Burial Ground.

Water travel times through the vadose zone were calculated using characteristic curves developed for Hanford sediments, assuming that unit gradient conditions prevail beneath the burial ground. Soil moisture characteristic curves describe the relationships between water content, water potential, and unsaturated hydraulic conductivity. The unsaturated hydraulic conductivity values were calculated from the measured saturated hydraulic conductivity (95 m/day) and the water content versus water potential data for well 299-E33-30 using the method of van Genuchten (1978; 1985). The resulting characteristic curves, plotted in Figure 4.1, indicate that increasing water content results in increasing unsaturated hydraulic conductivity values up to the limiting value of saturated hydraulic conductivity. For unit gradient conditions in the unsaturated zone, this recharge flux was assumed to equal the unsaturated hydraulic conductivity. The curves were used to determine the water content that results from the unsaturated hydraulic conductivity corresponding to the assumed recharge rates of 0.1, 0.5, and 6.0 cm/yr. The water content was then used to calculate the pore-water velocity through the 46-m-thick vadose zone beneath the 218-E-12B Burial Ground. Table 4.1 shows the water content, pore-water velocity, and vadose zone travel time for selected fluxes through the 46-m-thick vadose zone based on 299-E33-30 well data (Bjornstad 1990). The estimated groundwater travel times are 50 yr for the 6-cm/yr recharge case, 475 yr for the 0.5-cm/yr recharge case, and 2,146 yr for the 0.1-cm/yr case.

**TABLE 4.1.** Volumetric Water Content, Pore-Water Velocity, and Water Travel Time for Three Recharge Rates Through the Burial Ground

	<u>Recharge Rate (cm/yr)</u>		
	<u>0.1</u>	<u>0.5</u>	<u>6.0</u>
Volumetric Water Content	0.0467	0.0519	0.0659
Pore-Water Velocity (cm/yr)	2.13	9.63	91.05
Water Travel Time (yr)	2146	475	50

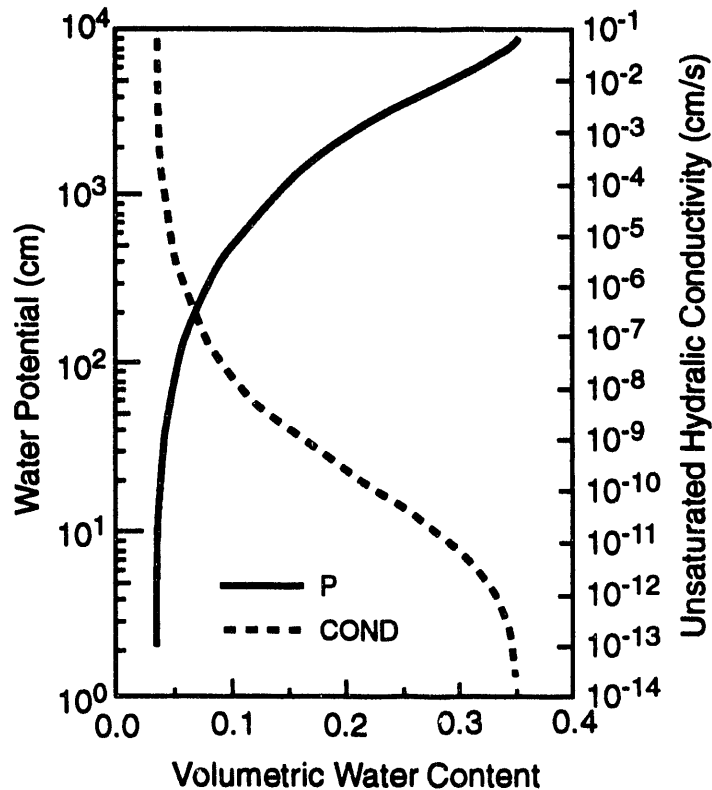


**FIGURE 4.1.** Moisture Retention Curves for Soil Samples from Well 299-E33-30 (Volumetric water content = water volume ÷ total volume; water potential = hydraulic head in cm H<sub>2</sub>O)

#### 4.3 GROUNDWATER FLOW MODELING

The CFEST code (Gupta et al. 1982; 1987) was applied to model groundwater flow in the unconfined aquifer and to generate streamlines and travel times that were used in the transport simulations. The CFEST code is being considered for acceptance as a Hanford Site standard for constructing models of the unconfined aquifer. Evans et al. (1988) describe selection of the CFEST code for application to the unconfined aquifer at the Hanford Site. Development and calibration of the CFEST model is described by Evans et al. (1988) and Jacobson and Freshley (1990). The conceptual model of the aquifer on which the CFEST model relies is based on information available in the early to mid-1980s. At that time, the top of the basalt formation in the vicinity of the 218-E-12B Burial Ground was believed to lie above the water table. Consequently, it was assumed that the Hanford formation was not saturated beneath the burial ground.

Today, as a result of this and other recent studies, the basalt is known to exhibit a saddle-type topography, with a trough running northwest to southeast underlying the 218-E-12B Burial Ground (see Figure 2.3). In addition, the water level in this part of the unconfined aquifer has risen during the past 10 yr because of increased discharges to B Pond, which is located southeast of the burial ground. When the liquid discharges to B Pond are discontinued during decommissioning of facilities in the 200-East Area, the water tables will drop and the basalt formation beneath the burial ground may lie above the water table. In the conceptual model of groundwater flow beneath the burial ground it was assumed that infiltrating water and leachate passing through the vadose zone would flow laterally across the basalt surface and enter the unconfined aquifer at the nearest location to the south of the discharge point.

#### 4.3.1 Groundwater Travel Times

This section summarizes the groundwater travel times that were calculated using the CFEST model. Groundwater flow in the unconfined aquifer was modeled to determine particle (i.e., water and lead) travel times to a well 100 m from the site, a well 5000 m from the site, and the Columbia River. Steady-state flow fields were simulated for site-wide recharge rates of 0.5 and 5.0 cm/yr (see Appendix A), which were intended to represent the range of long-term climatic conditions expected at the Hanford Site (Jacobson and Freshley 1990). Recharge conditions at specific locations on the Hanford Site may vary significantly from these site-wide averages depending on land use and vegetation cover. A recharge rate of 6 cm/yr was used to represent infiltration through the 218-E-12-B burial ground under maximum recharge conditions in the absence of a protective barrier. As noted previously, this is not substantially different from the site-wide recharge rate of 5 cm/yr, and provides consistency with studies already completed (Golder Associates, Inc. 1991). Installations with engineered infiltration barriers at Hanford would be expected to exhibit the lowest long-term recharge rates. Travel times to downgradient locations were determined using an effective porosity of 0.1 to calculate the pore-water velocity in groundwater for each specific discharge rate to the unconfined aquifer. The effective porosity value of 0.1 (10%) was determined in a previous study of aquifer characteristics

(Bierschenk 1959) and has been used for most subsequent model applications involving the unconfined aquifer at the Hanford Site (e.g., DOE 1987).

Streamlines from the burial ground to the river were generated using the CFEST aquifer model for each site-wide recharge rate considered in this analysis. Because the 1980s conceptual model of the aquifer predicted that Hanford formation sediments beneath the burial ground would be unsaturated, streamlines in the transport model could not begin directly below the burial ground. As a result, it was assumed that the difference in hydraulic conductivity between the sedimentary formation and the underlying basalt would cause water infiltrating downward through the vadose zone to flow across the top of the basalt until it reaches the unconfined aquifer. The basalt formation beneath the burial ground slopes toward the south. Therefore, several locations to the south of the burial ground were selected for the transport model as probable points where infiltrating water could enter the unconfined aquifer.

Water table contours for the site-wide 5.0-cm/yr recharge case indicate that the water table would be higher than for present-day conditions. This would cause a groundwater divide to develop in the low-gradient area south of Gable Mountain. The streamlines originating in the 200-East Area show that the groundwater flow direction would be generally northward toward the river through the gap between Gable Butte and Gable Mountain (Figure 4.2). Travel-time values for three locations along each streamline for a 5.0 cm/yr recharge rate are provided in Table 4.2. Groundwater travel times in the unconfined aquifer to the 100-m well range from 0.12 to 0.96 yr; times to the 5000-m well range from 1.8 to 3.3 yr; and times to the river range from 24 to 35 yr.

Groundwater flow in the site-wide 0.5-cm/yr case would be primarily from west to east across the entire Hanford Site, with streamlines intersecting the river at points along the site's eastern boundary (Figure 4.3). The lower water table would also cause more of the basalt to be unsaturated. In the CFEST model, the bottom of the unconfined aquifer is defined in some areas by the bedrock or basalt, whereas in other areas it is defined by a thick layer of low-permeability clay known as the Ringold Formation. In comparison with the Hanford formation sediments, the permeability of basalt or Ringold clay is several orders of magnitude lower. In the 0.5-cm/yr site-wide recharge case,

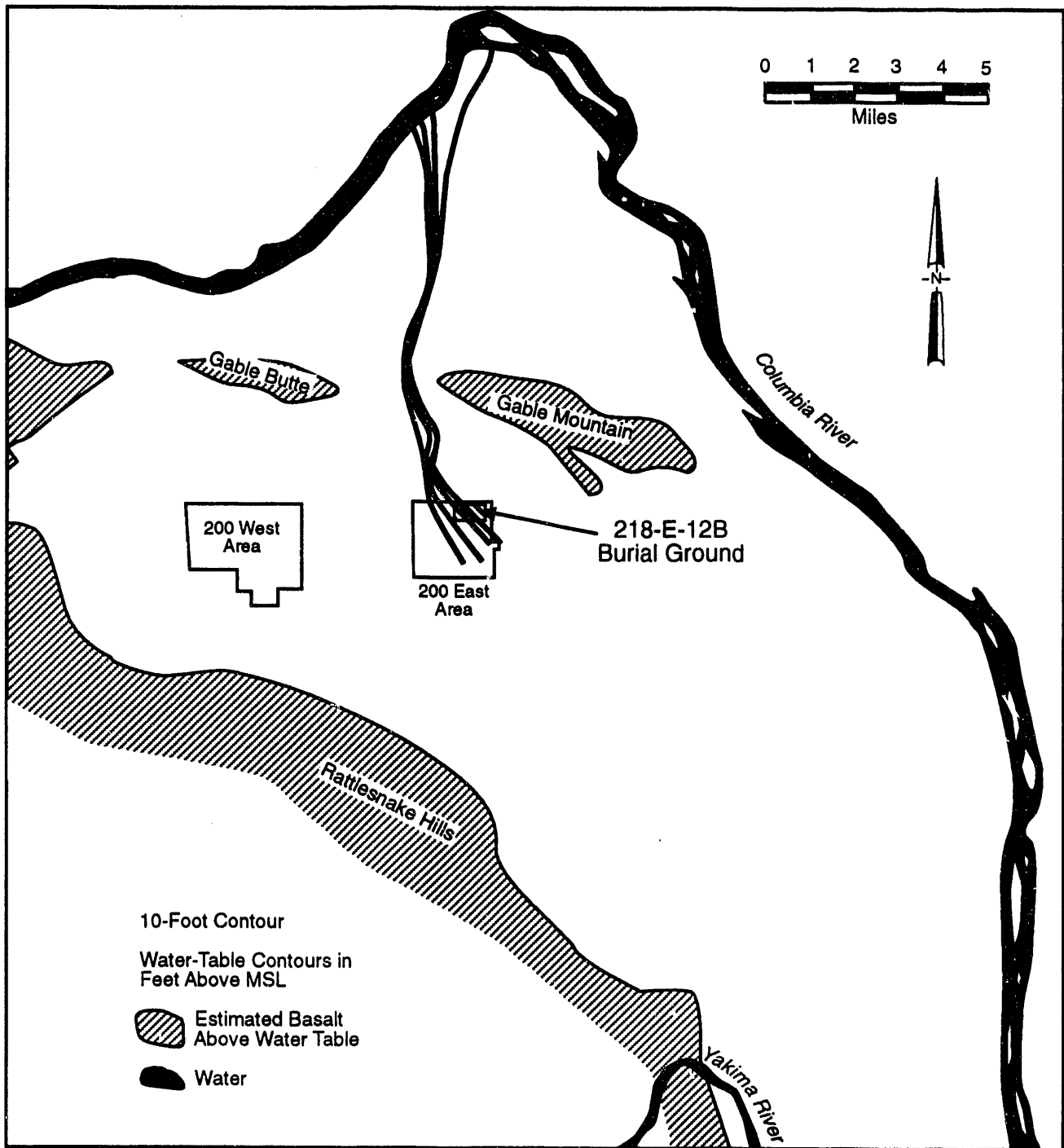


**FIGURE 4.2.** Streamlines from the 218-E-12B Burial Ground to the River for the 5.0 cm/yr Site-Wide Recharge Case

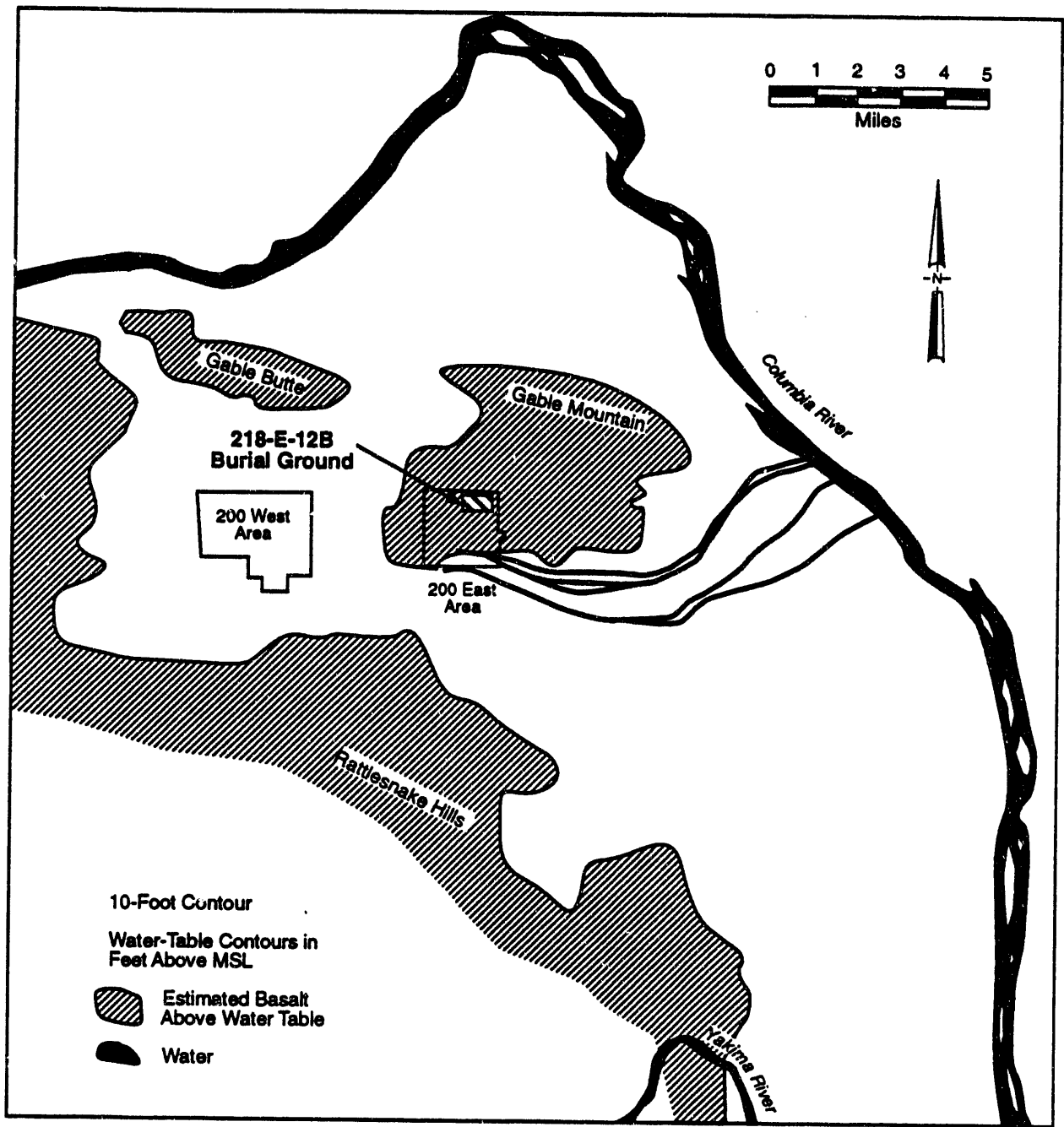


**FIGURE 4.3.** Streamlines from the 218-E-12B Burial Ground to the River for the 0.5-cm/yr Site-Wide Recharge Case

**TABLE 4.2. Travel Times Along Individual Streamlines in the Unconfined Aquifer for the 5.0-cm/yr Site-Wide Recharge Case**

Groundwater Travel Time to Downgradient Location (Yr)

<u>Streamline No.</u>	<u>100-m Well</u>	<u>5000-m Well</u>	<u>Columbia River</u>
1	0.63	1.82	34.4
2	0.95	1.98	24.5
3	0.12	2.43	35.4
4	0.25	3.30	32.0
5	0.14	2.73	25.8
6	0.96	2.06	24.3
Average:	0.51	2.39	29.4

most of the basalt and Ringold clays beneath the 200-East Area lie above the water table. Under these conditions, water infiltrating through the burial ground was assumed to flow south along the interface between the Hanford formation sediments and the low permeability underlying formation until it reaches the aquifer and enters a streamtube flowing toward the east or southeast (Figure 4.3). The streamlines (and travel times) are modeled beginning at points near the southern boundary of the 200-East Area.

Table 4.3 shows travel time values for three locations along each streamline based on the CFEST aquifer model for a site-wide recharge rate of 0.5 cm/yr. Groundwater travel times in the unconfined aquifer to the 100-m well range from 0.42 to 0.86 yr; times to the 5000-m well range from 33.4 to 105.0 yr; and times to the river range from 164 to 230 yr.

Aquifer simulations for the two site-wide recharge rates predicted markedly different groundwater flow patterns. This occurs because the site-wide recharge rate determines the hydraulic gradients within the unconfined aquifer and the level of the water table with respect to the basalt or Ringold clay that underlies the aquifer. This especially affects the estimated travel times to a water supply well at 5000 m and to the Columbia River. At the higher recharge rate, bedrock beneath the burial site is saturated, and groundwater is ultimately predicted to flow northward through the gap between Gable Butte and Gable Mountain. The travel time for water to reach a 100-m

**TABLE 4.3. Travel Times Along Individual Streamlines in the Unconfined Aquifer for the 0.5 cm/yr Site-Wide Recharge Case**

Groundwater Travel Time to Downgradient Location (Yr)

<u>Streamline No.</u>	<u>100-m Well</u>	<u>5000-m Well</u>	<u>Columbia River</u>
1	0.57	67.0	180
2	0.66	81.4	180
3	0.86	105.0	196
4	0.52	55.9	182
5	0.52	46.7	189
6	0.42	33.4	230
7	0.52	37.3	229
8	0.48	44.0	164
Average:	0.57	58.8	194

water supply well in this case is between 0.12 and 0.96 yr. However, the groundwater flow rate increases at distant points because it is subject to higher hydraulic gradients and hydraulic conductivities as it reaches the 5000-m well and discharges to the Columbia River. At the lower recharge rate, bedrock beneath the burial ground is exposed and nearby groundwater is predicted to flow toward the east or southeast. Groundwater travel to the 100-m well takes between 0.42 and 0.86 yr; however, the flow rate at downgradient locations becomes much slower as the hydraulic gradient decreases. Average travel times to the 100-m well predicted by the unconfined aquifer model for both recharge rates are virtually identical, at 0.51 and 0.57 yr for the high- and low-recharge cases respectively.

#### 4.3.2 Groundwater Velocity

The results of the two-dimensional groundwater flow model provide critical input to the one-dimensional TRANSS transport model calculations, because the estimated groundwater travel times are used to predict the groundwater (i.e., pore-water) velocity at the 100-m well, the 5000-m well, and the river. The groundwater velocity is critical to the transport calculation because it defines the volume of water available for dilution of the lead leaching from the burial ground. Therefore, the resulting lead

concentration in groundwater will be inversely proportional to the calculated groundwater velocity; that is, a higher groundwater velocity will result in lower lead concentrations in groundwater, and a lower groundwater velocity will result in higher lead concentrations in groundwater.

Because the one-dimensional TRANSS code could not accommodate the variable groundwater velocities predicted by the CFEST model at different distances from the burial ground, it was necessary to choose a single value to represent the groundwater velocity at all locations in order to achieve a fully consistent model. Average velocities for the 0.5- and 5.0-cm/yr recharge rates at the 100-m well were similar, at 175 and 197 m/yr, respectively. These values were also within the range predicted for the 5000-m well, which was 115 m/yr for a recharge rate of 0.5 cm/yr and 2073 m/yr for the 5.0-cm/yr case. Thus, the average velocity at the 100-m well, or 186 m/yr, was used as input for the TRANSS code in all cases. This value was consistent with the existing CFEST model of the Hanford Site, and it would be unlikely to overestimate the average flow rate at the 5000-m well (and thus underestimate the predicted lead concentration), particularly for the high recharge case.

#### 4.3.3 Limitations of the CFEST Groundwater Flow Model

The regional Hanford Site CFEST model generally reproduces the behavior of the unconfined aquifer at Hanford under current conditions, particularly for areas where the saturated sediments are thicker. However, the CFEST model does not have sufficient resolution to accurately predict local-scale behavior of the aquifer immediately beneath the 218-E-12B Burial Ground. Three conditions of the unconfined aquifer are described in this document: the current state of the aquifer (including recharge from site operations), its state under an enduring low site-wide recharge rate (0.5 cm/yr) in the absence of artificial recharge, and its state under an enduring high site-wide recharge rate (5 cm/yr). In the vicinity of the burial ground, groundwater currently flows west from B Pond, turning north through the gap between Gable Butte and Gable Mountain (see Figure 2.3). An evaluation of the regional geology for this study indicated that relatively high hydraulic heads measured north of the burial ground could result from groundwater recharging the unconfined aquifer from the Rattlesnake interbed (see Appendix A, Figure A.5

and section A.2.3.2). Based on hydraulic head measurements, the flow in this area north of the burial ground appears to be toward the southeast rather than the northwest. The high-recharge model simulation exhibits a similar flow through the gap between Gable Butte and Gable Mountain.

The low-recharge simulation predicts desaturation of basalt beneath the burial ground, in which case infiltrating water would be diverted along the contact to the south. Newcombe et al. (1972) documented the unconfined aquifer prior to the advent of significant artificial recharge resulting from Hanford operations, indicating that the pre-Hanford groundwater flow in the vicinity of the 200 Areas was generally from west to east, from the Yakima Ridge-Umtanum Ridge highland toward the Columbia River. Streamlines drawn in the vicinity of the 200 Areas form a streamtube with this general characteristic (Bjornstad 1990). A similar flow field might be expected to return with the decommissioning of artificial recharge sources at Hanford, such as B Pond and U Pond. Therefore, it is difficult to predict the exact direction of groundwater flow beneath the burial ground for any of the hypothetical aquifer conditions evaluated in this study, based on the present version of the CFEST model.

#### 4.4 LEAD TRANSPORT

Lead transport was estimated with the TRANSS code according to the general methodology described in Section 4.1. Recharge rates of 0.1 and 0.5 cm/yr, and a higher rate of 6 cm/yr as discussed by Golder Associates, Inc. (1991), were used for the analysis. These recharge rates were intended solely to represent flow through soil beneath the burial ground. The recharge rates of 5 cm/yr and 0.5 cm/yr used for the groundwater flow modeling in Section 4.3 represent a range of values for the Hanford Site as a whole based on a likely range for future climatic cycles, native vegetation, and human impact on soil surfaces across the Hanford Site.

Based on a 15-by-15-m (50-by-50-ft) storage area for each metal component, the 0.1 cm/yr recharge rate results in 232 L/yr of water that is assumed to pass through the buried waste and fully dissolve any lead up to the solubility limit. The 0.5-cm/yr recharge rate results in 1161 L/yr of water, and the 6.0-cm/yr recharge rate results in 13,935 L/yr of water that are

available to dissolve metal up to the solubility limit for each metal component. Consequently, at the higher recharge rate there is a greater volume of water available to dissolve lead from the wastes, and a greater quantity of lead is released to the subsurface soil and water.

Transport simulations in the unconfined aquifer require information on the aquifer dimensions in the area of interest. Previous analyses of shallow-land disposal using the methods employed in this study (DOE 1987; 1989) have evaluated locations on the Hanford Site that were overlying the unconfined aquifer, rather than the basalt formation that rises above the water table beneath the 218-E-12B Burial Ground (Figure 2.3). These studies assumed a 5-m thickness for the contaminated aquifer, which corresponded to the assumed use of a 5-m screened interval in a downgradient water supply well. Because of the thin saturated thickness of the aquifer in the vicinity of the burial ground, a shallower screened interval and aquifer thickness of 2.5 m was more appropriate for this analysis. A review of available field data (Section 2.3) estimated the saturated thickness near the burial ground at between 0.6 and 1.3 m. Therefore, it may be unreasonable to assume the existence of 5 m of saturated aquifer thickness at a distance of 100 m. For consistency, a 2.5-m screened interval was also used at the 5000-m well.

Both "best estimate" (0.3 mg/L) and "conservative" (0.55 mg/L) solubility limits were recommended for lead in Hanford groundwater, as described in Section 3.5 of this report. These solubilities, together with the assumed recharge rates and lead inventory estimates, determine the total release time for lead from the waste components. Multiplying the solubility by the annual water flux past each component yields the annual flux of lead into the soil column for each component (Table 4.4). The total annual quantity of lead released from the burial ground was estimated by multiplying the annual release per component by the number of components in the disposal array. Total release times for lead from both average and heavy units represent the times required to completely dissolve lead in the components, and these values range from  $2.3 \times 10^7$  to  $6.5 \times 10^9$  yr (Table 4.5). Consequently, extremely long release times are predicted from lead components in the burial ground.

**TABLE 4.4. Annual Flux of Lead into the Soil Column Beneath the 218-E-12B Burial Ground**

<u>Recharge Rate (cm/yr)</u>	<u>Lead Released to Soil (Grams per Component per Year)</u>		
	<u>0.1</u>	<u>0.5</u>	<u>6.0</u>
<u>Solubility</u>			
Best Estimate	0.070	0.348	4.181
Conservative	0.128	0.639	7.664

**TABLE 4.5. Total Estimated Release Times (in Years) for Lead from Components Disposed at the 218-E-12B Burial Ground**

<u>Component Mass</u>	<u>Solubility</u>	<u>Recharge Rate (cm/yr)</u>		
		<u>0.1</u>	<u>0.5</u>	<u>6.0</u>
Average	Best Estimate	3.3E+09	6.5E+08	5.4E+07
	Conservative	1.8E+09	3.6E+08	2.3E+07
Maximum	Best Estimate	6.5E+09	1.3E+09	1.1E+08
	Conservative	3.6E+09	7.1E+08	5.9E+07

After the metal is in solution, TRANSS models mass transport in the streamtube as described in Section 4.1 of this report. The streamtube width was based on the diagonal length through the waste disposal area (21.6 m for a single component and 461 m for 120 components), and the streamtube height in the aquifer was based on a 2.5-m mixing depth. During transport, a portion of the dissolved lead was assumed to adsorb to soil in the geologic units underlying the burial site according to the distribution coefficient ( $R_d$ ) described in Section 3.3.3 of this report. This process would retard or delay the rate at which the lead would otherwise flow through the vadose zone and aquifer in comparison with the groundwater travel times. Groundwater concentrations were calculated at wells located 100 m and 5000 m from the burial site, and the total annual flux was calculated for discharges to the Columbia River.

#### 4.5 LEAD CONCENTRATIONS

The results of the transport modeling for lead migration appear in Table 4.6, which shows lead concentrations (in mg/L and ppb) at the downgradient well locations and lead discharges to the river (in g/yr) for each source term at three different recharge rates. The "best estimate" and "conservative" transport cases incorporated the geochemical parameters discussed in Section 3.4 and listed in Table 3.7. For a single maximum component source, at the lower recharge rates of 0.1 and 0.5 cm/yr, concentrations at the 100-m and 5000-m wells ranged from  $7 \times 10^{-5}$  to  $6.4 \times 10^{-4}$  mg/L, and discharge to the Columbia River ranged from 0.07 to 0.64 mg/yr. The maximum concentrations and discharge rates peaked at times on the order of hundreds of thousands to millions of years and remained constant for millions of years thereafter (Table 4.7).

The values reported in Table 4.7 represent the time required for lead to travel through the vadose zone to the unconfined aquifer plus travel time in the aquifer to an indicated downgradient location. Transport through the vadose zone to the unconfined aquifer is the product of the groundwater travel time (see section 4.2) and the lead retardation factors reported in Table 3.7. Vadose zone travel times ranged from  $8.6 \times 10^7$  yr in the "best estimate" case at 0.1 cm/yr recharge to  $2.4 \times 10^5$  yr in the "conservative" case at 6 cm/yr recharge. As indicated by the corresponding values in Table 4.7, the travel time from the point at which lead entered the aquifer to the 100-m well was a relatively insignificant fraction of the total transport time.

The peak concentration in groundwater for a single component was estimated to be 0.0076 mg/L in the 6-cm/yr recharge case. The peak concentration is established after approximately 242,000 yr and remains constant for several million years thereafter (Figure 4.4). The same peak concentration of 0.0076 mg/L was predicted at the 5000-m well, although it does not occur until 340,000 yr after burial. A maximum lead flux of 7.7 g/yr to the Columbia River was estimated beginning at about 740,000 yr for the "conservative" case and 6-cm/yr recharge. Under these conditions the lead concentration in river water would be  $7.7 \times 10^{-11}$  mg/L, based on an annual average flow rate of  $1 \times 10^{14}$  L/yr. The maximum flux is approximately equal to the annual amount of lead assumed to leach from the component (7.7 g/yr in

**TABLE 4.6. Peak Lead Concentration in Downgradient Groundwater Wells or Maximum Flux of Lead to the Columbia River as a Function of Release Conditions from the 218-E-12B Burial Ground**

Receptor Location	Recharge Rate	Transport Case <sup>(a)</sup> Parameter Estimates	Downgradient Groundwater Concentration, mg/L or (ppb)		
			Source Term		
			Single Component	Multiple Components in a 4-x-30 Array	
			Max Mass Pb ( $4.5 \times 10^5$ kg)	Max Mass Pb ( $5.5 \times 10^7$ kg)	Avg Mass Pb ( $2.7 \times 10^7$ kg)
100-m Well	0.1 cm/yr	Best Estimate	7.0E-05 (0.07)	3.9E-04 (0.39)	3.9E-04 (0.39)
		Conservative	1.3E-04 (0.13)	7.2E-04 (0.72)	7.2E-04 (0.72)
	0.5 cm/yr	Best Estimate	3.5E-04 (0.35)	2.0E-03 (2.0)	2.0E-03 (2.0)
		Conservative	6.4E-04 (0.64)	3.6E-03 (3.6)	3.6E-03 (3.6)
	6.0 cm/yr	Conservative	7.6E-03 (7.6)	4.3E-02 (43.)	4.3E-02 (43.)
	5000-m Well	0.1 cm/yr	Best Estimate	7.0E-05 (0.07)	3.9E-04 (0.39)
Conservative			1.3E-04 (0.13)	7.2E-04 (0.72)	7.2E-04 (0.72)
0.5 cm/yr		Best Estimate	3.5E-04 (0.35)	2.0E-03 (2.0)	2.0E-03 (2.0)
		Conservative	6.4E-04 (0.64)	3.6E-03 (3.6)	3.6E-03 (3.6)
6.0 cm/yr		Conservative	7.6E-03 (7.6)	4.3E-02 (43.)	4.3E-02 (43.)
			River Flux (g/yr)		
River	0.1 cm/yr	Best Est.	7.0E-02	8.4E+00	8.4E+00
		Conservative	1.3E-01	1.5E+01	1.5E+01
	0.5 cm/yr	Best Est.	3.5E-01	4.2E+01	4.2E+01
		Conservative	6.4E-01	7.7E+01	7.7E+01
	6.0 cm/yr	Conservative	7.7E+00	9.2E+02	9.2E+02

(a) "Best estimate" and "conservative" transport cases include the corresponding geochemical parameters listed in Table 3.6.

**TABLE 4.7. Time of Peak Lead Concentration in Downgradient Groundwater Wells or Maximum Flux of Lead to the Columbia River as a Function of Release Conditions from the 218-E-12B Burial Ground**

Receptor Location	Recharge Rate	Transport Case <sup>(a)</sup> Parameter Estimates	Time to Reach Peak Well Concentration or Maximum Flux to the Columbia River (millions of years)		
			Source Term		
			Single Component	Multiple Components in a 4-x-30 Array	
			Max Mass Pb ( $4.5 \times 10^5$ kg)	Max Mass Pb ( $5.5 \times 10^7$ kg)	Avg Mass Pb ( $2.7 \times 10^7$ kg)
100-m Well	0.1 cm/yr	Best Estimate	85.8	85.8	85.8
		Conservative	10.3	10.3	10.3
	0.5 cm/yr	Best Est.	19.0	19.0	19.0
		Conservative	2.2	2.2	2.2
	6 cm/yr	Conservative	0.24	0.24	0.24
5000-m Well	0.1 cm/yr	Best Est.	85.9	85.9	85.9
		Conservative	10.4	10.4	10.4
	0.5 cm/yr	Best Est.	20.0	20.0	20.0
		Conservative	2.4	2.4	2.4
	6 cm/yr	Conservative	0.34	0.34	0.34
River	0.1 cm/yr	Best Est.	86.2	86.2	86.2
		Conservative	10.8	10.8	10.8
	0.5 cm/yr	Best Est.	23.0	23.0	23.0
		Conservative	2.8	2.8	2.8
	6 cm/yr	Conservative	0.74	0.74	0.74

(a) "Best estimate" and "conservative" transport cases include the corresponding geochemical parameters listed in Table 3.6.

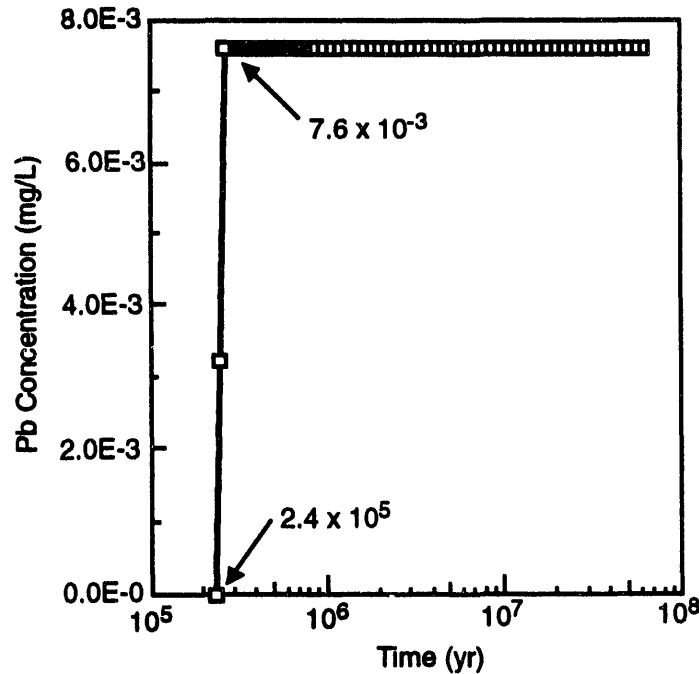


**FIGURE 4.4.** Concentration of Lead in Groundwater at the 100-m Well -- Maximum Single Disposal Unit, "Conservative" Transport Case, 6-cm/yr Recharge

Table 4.4) indicating that mass balance was maintained in the simulations after equilibrium conditions were established.

For the component arrays, groundwater concentrations and releases to the river were calculated for 120 components having either an average or a maximum total mass of lead (Table 4.6). Lower lead concentrations at downgradient wells were predicted for the lower recharge rates because a smaller volume of water would contact the waste components annually. Concentrations in groundwater ranged from  $3.9 \times 10^{-4}$  to  $3.6 \times 10^{-3}$  mg/L for both array sources. Discharges to the Columbia River for the lower recharge cases ranged from 8.4 to 77 g/yr. Plots of concentration versus time at the 100-m well for the maximum inventory array are shown in Figures 4.5 and 4.6 for the 0.1- and 0.5-cm/yr recharge cases, respectively.

As with the single component, the highest concentrations and discharges for component arrays were predicted in the 6-cm/yr recharge case. Peak concentrations at the wells were approximately 0.043 mg/L for the maximum array and average array sources (Figures 4.7 and 4.8). Peak discharges to the

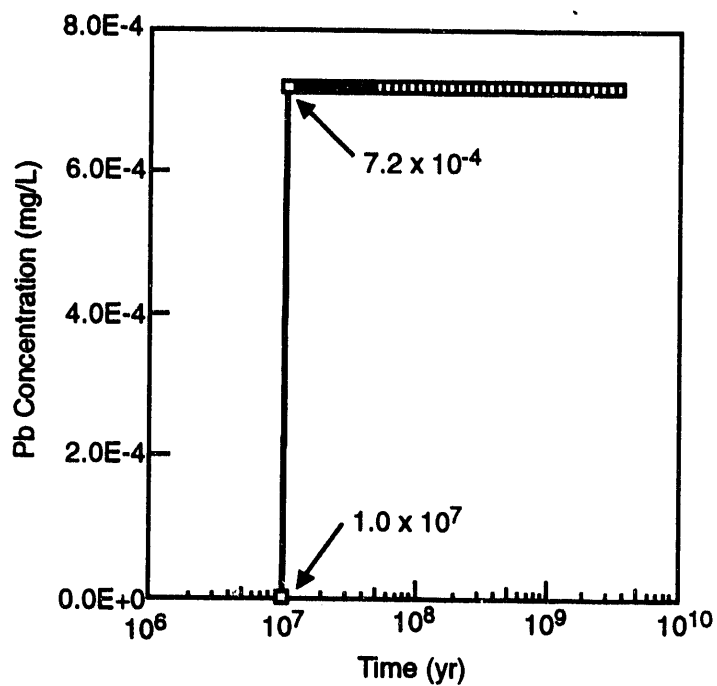


**FIGURE 4.5.** Concentration of Lead in Groundwater at the 100-m Well -- Maximum Array of Disposal Units, "Conservative" Transport Case, 0.1-cm/yr Recharge

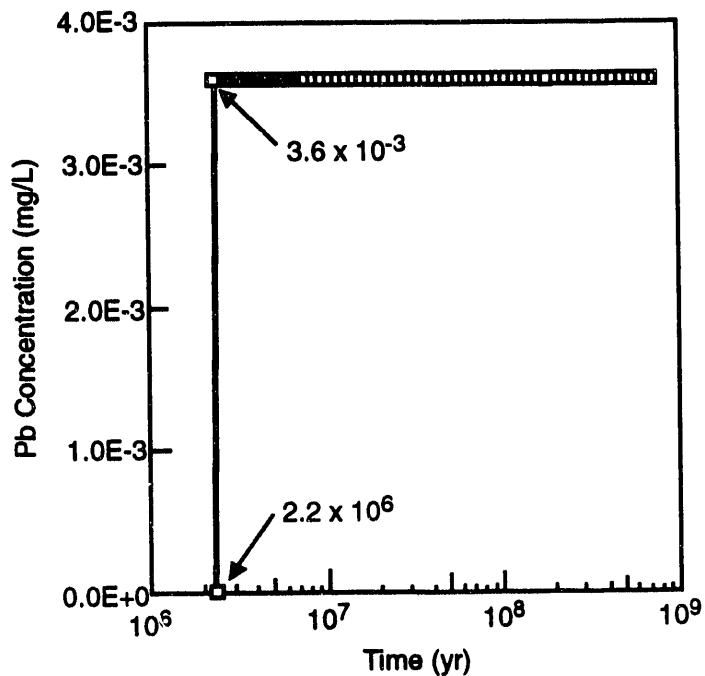


**FIGURE 4.6.** Concentration of Lead in Groundwater at the 100-m Well -- Maximum Array of Disposal Units, "Conservative" Transport Case, 0.5-cm/yr Recharge

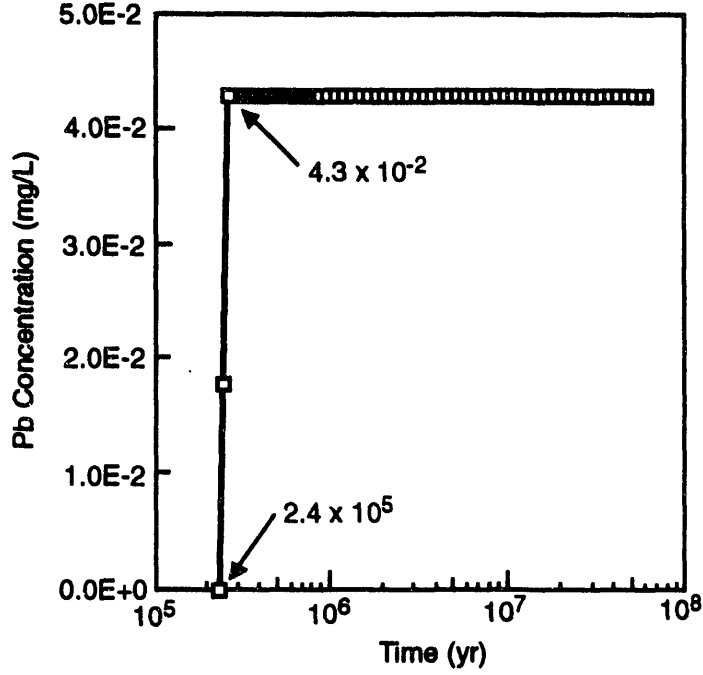


**FIGURE 4.7.** Concentration of Lead in Groundwater at the 100-m Well -- Maximum Array of Disposal Units, "Conservative" Transport Case, 6-cm/yr Recharge

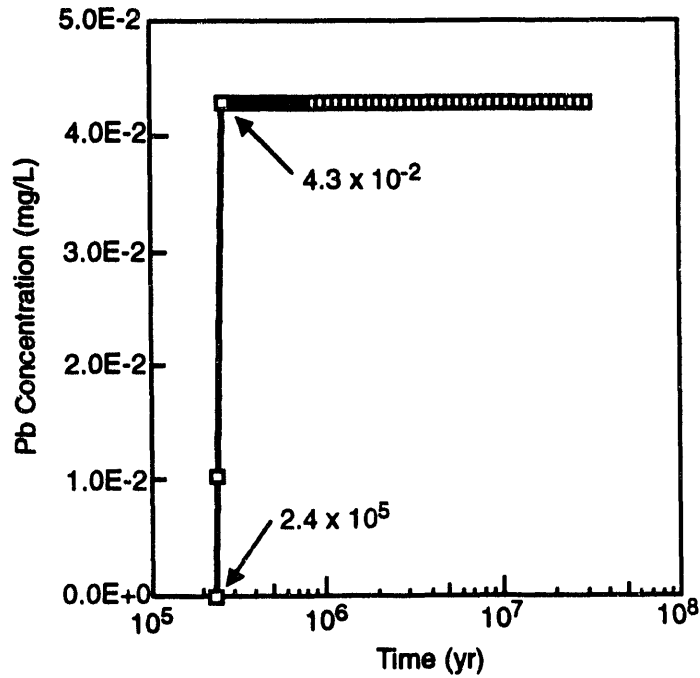


**FIGURE 4.8.** Concentration of Lead in Groundwater at the 100-m Well -- Average Array of Disposal Units, "Conservative" Transport Case, 6-cm/yr Recharge

Columbia River were approximately 920 g/yr for both sources. Again, this is approximately equal to the quantity of lead leached from the component arrays annually. Peak groundwater concentrations occurred at the same times as for the single-component source terms. Note the relatively longer times required to reach the peak concentrations (2 million to 86 million yr) in the lower recharge cases compared with the 6-cm/yr case.

Predicted groundwater concentrations for the arrays containing "average" and "maximum" size components were similar in this analysis because of the assumption that release of lead from the waste always occurs at the solubility limit of lead in water for the total amount of water passing through the burial array as recharge. The size of the individual components, therefore, had no effect on the annual quantity of saturated lead solution leaching from the burial ground. The difference between the two sources would be that lead in the average mass array would be depleted in a shorter time than lead in the maximum mass array.

#### 4.6 DISCUSSION

The results of this analysis are based on a relatively simplified theoretical model, and on available information about the physical and chemical environment surrounding the burial ground. There are areas of uncertainty, both in the model itself and in the parameters used by the model to produce quantitative estimates of lead concentrations in ground- and surface waters downgradient from the burial site. An attempt has been made as part of this study to determine accurate values for parameters that are critical to the analysis (lead solubility and adsorption coefficients, for example). However, there are elements less amenable to laboratory or field analysis that influence the results obtained from the model.

One element of uncertainty in the transport calculations is the nature of the future hydrological environment, particularly the direction in which groundwater in the unconfined aquifer will flow in the absence of artificial recharge from the 200 Areas. This uncertainty is reflected in the transport model by the cross-sectional area used to represent the streamtube. The streamtube approach is a simplified representation of the water column that would transport dissolved lead from the burial ground to the river. The model

used for this analysis did not consider lateral dispersion of lead within the streamtube; therefore, its width and depth were assumed to be constant along the entire length. The streamtube dimensions assumed for the transport model directly affected the estimated lead concentrations in groundwater because, at a given recharge rate, they determined the volume of water into which the lead was ultimately diluted. In this model, the depth of the streamtube was set at a constant 2.5 m, and the width was taken to be the longest dimension of the burial ground perpendicular to the predicted direction of groundwater flow. Potential widths of the streamtube for the 120-component array ranged from 61 m along the narrow axis of the burial ground to 461 m along the diagonal.

For all simulations, the diagonal dimension of the 4-by-30 array (461 m) was used for the streamtube width, which is consistent with the results of the CFEST model (discussed in section 4.3) and the current regional hydrology (discussed in section 2.3), which predicts groundwater flow to be generally north or south and roughly perpendicular to the diagonal of the burial ground (Figure 2.3). However, the limitations of the CFEST model, described in Section 4.3.3, imply that groundwater could flow in alternative directions under some future conditions. Although it is less probable than the north or south direction predicted by the model, flow in an alternative direction would result in a higher estimated groundwater concentration for lead because the corresponding width of the streamtube in the transport model would be reduced. A smaller streamtube would decrease the quantity of water in which leachate from the burial ground would be diluted; therefore, lead concentrations in the groundwater would increase in proportion to the reduction in streamtube width.

The values in Table 4.6 can be used to determine the predicted lead concentration for any future groundwater flow direction by multiplying them by the ratio of the burial ground diagonal length (461 m) to the dimension perpendicular to the assumed flow direction. The maximum estimate obtained by this procedure would be for a flow direction from west to east along the length of the burial ground. In this case, the Table 4.6 values would be multiplied by the ratio of the burial ground diagonal length (461 m) to its width (61 m) or a factor of 7.6. The ratio corresponding to any other assumed groundwater flow direction would be smaller. However, the estimated travel times to downgradient locations, the quantity of lead leached from the burial

ground, and the estimated maximum mass of lead entering the Columbia River annually would be independent of the configuration of the streamtube.

Another major source of uncertainty in this analysis is the very long time span required for transport of lead to the groundwater and to downgradient locations, because the future geologic and hydrologic environment in the vicinity of the burial ground may be substantially different from its present configuration. DOE (1987) reports on studies by Craig<sup>2</sup> and Craig and Hanson (1985) that describe the potential for ice-age flooding that could affect the Hanford Site as a result of climatic change over approximately the next 50,000 yr. Those studies documented evidence concerning the effects of flooding due to the catastrophic release of ice-impounded water from Lake Missoula. During the floods, it was estimated that as much as 2000 km<sup>3</sup> of water flowed through the Pasco Basin over a period of a few weeks. A relatively weak ice age that is predicted in about 15,000 yr would not likely generate flooding of this volume; therefore, DOE (1987) does not consider glacial flooding as a potential release mechanism for hazardous wastes buried at the Hanford Site during the next 10,000 yr. However, those studies predicted a recurrence interval of 40,000 to 50,000 yr for major flooding events of this magnitude, which is substantially shorter than the time required for lead to reach the water table in this analysis.

The possible fate of buried wastes was also examined by the studies. The first wave of a major glacial flood could scour the existing sedimentary deposits to a considerable depth; however, the sediments would likely be redeposited in the Pasco Basin. The flood waters could potentially scour out the metal components, the soil column, and portions of the aquifer as well. Any lead in solution would also be diluted by a significant volume of flood water. With regard to disposal of radioactive wastes at Hanford, DOE (1987) concluded that "...the radiological consequences of a glacial flood would not appear important in contrast to the effects of the flood itself." Although lead is a nonradiological hazardous waste, a similar conclusion would seem reasonable for lead wastes in the event of such a flood. The residual impact

---

<sup>2</sup> Craig, R. G. 1983. "Analysis of Ice-Age Flooding from Lake Missoula." Unpublished report, Kent State University, Kent, Ohio.

of lead in the waste components would be expected to be insignificant compared with the effects of the flood itself.

#### 4.7 SOURCES OF CONSERVATISM IN THE GROUNDWATER AND TRANSPORT MODELS

This evaluation was conducted using a relatively simple screening model to obtain order-of-magnitude estimates for lead concentrations in groundwater. As a result, the analyses of groundwater flow and lead transport were necessarily simplified in several respects to make the simulation possible. Although the simulated groundwater flow directions, as described in sections 4.3.3 and 4.6, did not produce the most conservative result, the overall evaluation was conservative because of the nature of the model and the assumptions made regarding other parameters. The major sources of conservatism in the analysis are described in the following sections.

##### 4.7.1 Infiltrating Water at the Solubility Limit of Lead

All water infiltrating the soil profile associated with each metal component (i.e., a 15-by-15-m area) was assumed to come into contact with the metal and reach equilibrium with the lead source. This results in solution entering the vadose zone at the solubility limit of lead. In reality, not all infiltrating water would be expected to contact the components, and neither would all water contacting the components be exposed to lead or reach the solubility limit for lead in solution. Although these assumptions simplified the simulation, they resulted in higher predicted release rates and downgradient water concentrations than would actually be expected.

##### 4.7.2 Hydraulic Impact of a Resource Conservation and Recovery Act Barrier

This analysis did not account for the effect of a Resource Conservation and Recovery Act (RCRA) barrier that may be placed over the metal components in the burial ground, nor was water flow simulated in the backfill material that would surround and overlie the metal components. An RCRA barrier has a design life span of approximately 30 yr and would act as an underground umbrella to shield the waste from large amounts of infiltrating water. Any water shed by the RCRA barrier would be redirected to soils outside the waste disposal area, thus reducing the amount of infiltration that could contact the waste form as long as the barrier remains intact. The clay material used for

the barrier is often characterized by its saturated hydraulic conductivity,  $K_s$ . The barrier is designed to divert infiltrating water at recharge rates that exceed  $K_s$ , and would be expected to transmit water at recharge rates lower than, or equal to,  $K_s$ .

Excluding the hydraulic influence of a RCRA barrier in this analysis of water flow and lead transport is expected to overestimate both the quantity of water contacting the waste and the concentration and mass flux of lead in the water carried away from the burial site during the functional life of the barrier. Therefore, the models employed in this analysis should be conservative for the early post-disposal period, particularly at the 6-cm/yr recharge rate, because the influence of an RCRA barrier would increase at the higher infiltration rate. In reality, the processes that would act to degrade or alter the performance of the RCRA barrier occur over very long time periods, and the effective life of the barrier *in situ* could be considerably greater than its engineered design life. Because the potential influence of the barrier is difficult to predict over the time span required for release of lead from the components, the hydraulic influence of an RCRA barrier was not considered as part of this analysis.

#### 4.7.3 Recharge Rate with a Protective Barrier

A protective multilayered soil/rock barrier system is also being studied and designed for use in shallow-land burial sites at Hanford. This is a different design than the RCRA clay cover discussed in section 4.7.2, and the protective barrier may be installed either with or without the RCRA barrier (which has a shorter design life). The protective barrier could virtually eliminate water infiltration. In addition, it was designed to minimize wind and water erosion and to provide a deterrent to animal or human intrusion over the long term. Analyses conducted to date have shown that a barrier constructed with appropriate materials should not permit any deep recharge at double the rates used in these scenarios. However, the present estimate of recharge through the barrier (i.e., 0.1 cm/yr) was used for transport modeling because of three issues: 1) field measurement instruments always introduce measurement error (thus, absolute zero recharge cannot be measured); 2) computer simulations of barrier performance always introduce round-off and truncation error (thus, absolute zero recharge cannot be based solely on

computer simulation); and 3) uncertainty in stochastic aspects of both the climate and barrier performance give rise to low-probability scenarios, such as sequentially occurring high-precipitation years, which may cause water to drain through the barrier system. This scenario was hypothesized to result in 5 cm of recharge over a 100-yr period, which amounts to an average of 0.05 cm/yr of long-term recharge. This is the performance objective of the barrier system; therefore, use of 0.1 cm/yr as the estimated recharge rate through the protective barrier in the model represents a conservative treatment of this low-probability scenario during the life of the barrier. The 0.5-cm/yr and 6.0-cm/yr recharge rates used to represent long-term climatic conditions at the burial site in the absence of an engineered barrier may also be considered to represent the situation that would occur if a barrier were present, but it had degraded over time.

#### 4.7.4 Omission of Lateral or Transverse Dispersion

In reality, lateral dispersion within the vadose zone could result in lower peak concentrations of lead in solution compared with those predicted by the one-dimensional streamtube model used for this analysis. This would decrease the concentration of lead in the groundwater at some points in the unconfined aquifer and increase it at other locations. Therefore, the long-term release scenario could result in some vadose zone water reaching the water table at a concentration below the solubility limit. This analysis was conservative in the assumption that all vadose zone water will move vertically downward and not mix laterally with the adjacent clean water, eventually reaching the water table at the maximum solubility concentration for lead.

Lateral dispersion within the unconfined aquifer could also result in lower peak concentrations of lead at the 5000-m well and in water discharging to the Columbia River, although it would not affect the total quantity of lead entering the river annually. Currently, the streamtube model embodied in the TRANSS code neglects all transverse or lateral dispersion. Estimated lead concentrations at a 100-m well would probably not be reduced significantly by using a multidimensional transport and dispersion model of the unconfined aquifer because of the proximity of the well to the waste site. However, omission of lateral dispersion probably resulted in conservative estimates for lead concentrations at the more distant points.

#### 4.7.5 Areal Extent of Basalt and Ringold Formation Above the Water Table

Several uncertainties exist in the current model of the unconfined aquifer, making it difficult to estimate the areal extent of basalt and Ringold Formation above the water table in the vicinity of the 218-E-12B Burial Ground. The uncertainty in the model for the burial ground is due to the limited information available on water levels and on the geometry of the geologic units in the area, as well as the current lack of spatial resolution in the groundwater flow model.

Currently, the waste water disposal operation at B Pond has a significant influence on the water table in the vicinity of the 218-E-12B Burial Ground. In this area of the site, the unconfined aquifer is located in the lowest sequence of the Hanford formation and is estimated to be less than 3-m thick. A comparison of pre-Hanford water levels (Newcombe et al. 1972) to current water levels (Evans et al. 1988) in the area would seem to indicate that the presence of groundwater in the Hanford formation immediately below the burial site is a result of liquid discharges to B Pond. When the liquid discharges to B Pond are discontinued as a result of decommissioning of 200-East Area facilities, the water table will drop and the basalt formation beneath the burial ground should again be above the water table. The bottom of the Hanford formation is considered to be the base of the unconfined aquifer in the immediate vicinity of the burial ground because the saturated hydraulic conductivity of the underlying basalt is several orders of magnitude lower than that of gravels in the Hanford formation. Therefore, the basalt is assumed to be relatively impermeable compared with the sedimentary strata overlying it. The current model was established in the mid-1980s, and only recently have data near the burial ground been available to improve our knowledge of the interface between these formations in the area.

The current model of groundwater flow in the unconfined aquifer, which is based on the CFEST code, is two-dimensional and does not incorporate variations in the vertical dimension. The model is also regional in scale and does not contain sufficient resolution to represent local features in the vicinity of the burial ground. It was designed to reproduce groundwater flow and contaminant transport phenomena to the south and east of the separations facilities located in the 200-East Area, and to the north of facilities

located in the 200-West Area. The principal inconsistency with newly available data has been the model's prediction of a significant expanse of basalt above the water table. Additional conservatism is added to the TRANSS transport calculations because of the approach taken to estimate the time required for infiltrating water to move downslope off the basalt surface and drain into the unconfined aquifer. We have assumed a zero travel time for water to traverse the relatively impermeable surface of the bedrock and enter the unconfined aquifer. This conservative approach to estimating a segment of the overall travel time from source to downgradient locations has been taken because of uncertainty about the areal extent of basalt above the water table.

A related issue is the rate at which aquifer thickness increases as groundwater moves away from the burial ground. The aquifer depth determines, in part, the volume of groundwater that dilutes the lead in recharge water percolating through the vadose zone. Recent information indicates that the saturated zone immediately beneath the burial ground is approximately 1 m deep, whereas the depth is known to exceed 5 m at many downgradient locations. Because of the proximity of the 100-m well to the burial ground, an average aquifer (mixing) depth of 2.5 m was assumed for that location, and it was also applied to the 5000-m well for consistency. This approach, therefore, was likely to produce conservative (i.e., high) estimates for the lead concentrations in groundwater, particularly at the 5000-m well location for the 6-cm/yr recharge rate.

#### 4.7.6 Estimates of the Distribution or Adsorption Coefficient

Adsorption of lead on soil as simulated for this analysis was conservative for several reasons. The  $R_d$  values determined in this study were found to be a function of the equilibrium solution concentration. As the equilibrium solution concentrations of Pb increased, the  $R_d$  values decreased according to Equation (3.5). The  $R_d$  value selected to model lead transport for the "conservative" case was approximately half of that expected for lead adsorption near the solubility limit of cerussite (which is theoretically the highest concentration of lead possible for this system). Based on the mass of lead disposed and the available cation exchange sites in the vadose zone and aquifer sediments, solution lead concentrations near the solubility limit should only exist near the source and through part of the vadose zone. As

water percolates through the soil column and into the aquifer, adsorption on sediments and dilution by groundwater would decrease the lead concentrations at downgradient locations. For example, the appropriate  $R_d$  estimated from Equation (3.5) for a solution saturated with cerussite ( $300 \mu\text{g/L}$ ) would be  $1400 \text{ mL/g}$ , whereas  $1200 \text{ mL/g}$  was actually used in the "conservative" transport case. For an equilibrium solution at  $1 \mu\text{g/L}$  of lead, the appropriate  $R_d$  value would be  $9550 \text{ mL/g}$ . Consequently,  $R_d$  values would be expected to increase as the distance from the source increases during the time when lead is actively dissolving from the components. However, lead transport was modeled for the "conservative" case as if the lower  $R_d$  value (determined for a solution concentration of  $300 \mu\text{g/L}$ ) was appropriate at all locations. For the "best estimate" case, an  $R_d$  value of  $10,000 \text{ mL/g}$  was used to represent an average for the entire transport path, although it was substantially lower than the maximum  $R_d$  values observed in the batch adsorption studies.

#### 4.8 SUMMARY

Estimates of lead migration from the burial ground and the conservative assumptions incorporated into the modeling are described in this section of the report. A peak groundwater concentration of  $0.043 \text{ mg/L}$  and a peak annual release of  $920 \text{ g/yr}$  to the Columbia River were estimated for  $6.0\text{-cm/yr}$  recharge in the "conservative" transport case. At the  $0.5\text{-}$  or  $0.1\text{-cm/yr}$  recharge rates, the predicted maximum groundwater concentrations and the annual quantity of lead reaching the river were significantly lower. The peak concentrations at all recharge rates were not predicted to occur for hundreds of thousands to millions of years. The results of the lead transport analyses indicated that a protective infiltration barrier on the surface of the 218-E-12B Burial Ground could have a significant impact on the concentrations that are eventually observed in groundwater, if it had a sufficiently long life span to reduce the infiltration rate for extended periods of time. However, it is unlikely that any engineered barrier would provide protection against water infiltration over the millions of years that lead will be leaching from the components. On this time scale, geologic events would be expected to transform the existing hydrogeology through tectonics, vulcanism, deposition, erosion, and other mechanisms.

## 5.0 REFERENCES

- Bierschenk, W. H. 1959. Aquifer Characteristics and Groundwater Movement at Hanford. HW-60601, Hanford Atomic Products Operation, General Electric Company, Atomic Energy Commission, Washington, D.C.
- Bjornstad, B. N. 1990. Geohydrology of the 218-W-5 Burial Ground, 200-West Area, Hanford Site. PNL-7336, Pacific Northwest Laboratory, Richland, Washington.
- Bjornstad, B. N., and S. Dudziak. 1989. 40 CFR 265 Interim Status Indicator-Evaluation Ground-Water Monitoring Plan for the 216-B-63 Trench. PNL-6862, Pacific Northwest Laboratory, Richland, Washington.
- Borghese, J. V., D. R. Newcomer, W. E. Cronin, and S. M. Goodwin. 1990. Hydrologic Testing at the Low-Level Burial Grounds, 1989. PNL-7333, Pacific Northwest Laboratory, Richland, Washington.
- Craig, R. G., and J. P. Hanson. 1985. Erosion Potential from Missoula Floods in the Pasco Basin, Washington. PNL-5684, prepared by Kent State University for Pacific Northwest Laboratory, Richland, Washington.
- Evans, J. C., D. I. Dennison, R. W. Bryce, P. J. Mitchell, D. R. Sherwood, K. M. Krupka, N. W. Hinman, E. A. Jacobson, and M. D. Freshley. 1988. Hanford Site Groundwater Monitoring for July Through December 1987. PNL-6315-2, Pacific Northwest Laboratory, Richland, Washington.
- Felmy, A. R., D. C. Girvin, and E. A. Jenne. 1984. MINTEQ: A Computer Program for Calculation of Aqueous Geochemical Equilibria. EPA/600/3-84-032 (NTIS PB84-157148), Prepared for the U.S. Environmental Protection Agency (Athens, Georgia) by Battelle, Pacific Northwest Laboratories, Richland, Washington.
- Golder Associates, Inc. 1991. Estimated Distribution of Water in Unsaturated Zone from Potential Releases from Submarine Reactor Compartments at the Hanford Site. WHC-MR-0266, Westinghouse Hanford Company, Richland, Washington.
- Graham, M. J., M. D. Hall, S. R. Strait, and W. R. Brown. 1981. Hydrology of the Separations Area. RHO-ST-42, Rockwell Hanford Operations, Richland, Washington.
- Gupta, S. K., C. T. Kincaid, P. R. Meyer, C. A. Newbill, and C. R. Cole. 1982. A Multi-Dimensional Finite Element Code for the Analysis of Coupled Fluid, Energy, and Solute Transport (CFEST). PNL-4260, Pacific Northwest Laboratory, Richland, Washington.

Gupta, S. K., C. R. Cole, C. T. Kincaid, and A. M. Monti. 1987. Coupled Fluid, Energy, and Solute Transport (CFEST) Model: Formulation and User's Manual. BMI/ONWI-660, Office of Nuclear Waste Isolation, Battelle Memorial Institute, Columbus, Ohio.

Jacobson, E. A., and M. D. Freshley. 1990. An Initial Inverse Calibration of the Groundwater Flow Model for the Hanford Unconfined Aquifer. PNL-7144, Pacific Northwest Laboratory, Richland, Washington.

Last, G. V., B. N. Bjornstad, M. P. Bergeron, D. W. Wallace, D. R. Newcomer, J. A. Schramke, M. A. Chamness, C. S. Cline, S. P. Airhart, and J. S. Wilbur. 1989. Hydrogeology of the 200 Areas Low-Level Burial Grounds--An Interim Report. PNL-6820, Pacific Northwest Laboratory, Richland, Washington.

Lum, W. E., J. L. Smoot, and D. R. Ralston. 1990. Geohydrology and Numerical Model Analysis of Groundwater Flow in the Pullman-Moscow Area, Washington and Idaho. Water-Resources Investigations Report 89-4103, U. S. Geological Survey, Tacoma, Washington.

Mullineaux, D. R., R. E. Wilcox, W. F. Ebaugh, R. Fryxell, and M. Rubin. 1978. "Age of the Last Major Scabland Flood of the Columbia Plateau in Eastern Washington." Quaternary Research 10:171-180.

Newcombe, R. C., J. R. Strand, and F. J. Frank. 1972. Geology and Groundwater Characteristics of the Hanford Reservation of the U.S. Atomic Energy Commission, Washington. U.S. Geological Survey Professional Paper 717, U.S. Geological Survey, Denver, Colorado.

Relyea, J. F. 1982. "Theoretical and Experimental Considerations for the Use of the Column Method for Determining Retardation Factors." Rad. Waste Man. and the Nucl. Fuel Cycle 3:115-130.

Relyea, J. F., Serne, R. J., and D. Rai. 1980. Methods of Determining Radionuclide Retardation Factors. PNL-3349, Pacific Northwest Laboratory, Richland, Washington.

Serne, R. J., and J. F. Relyea. 1983. "The Status of Radionuclide Sorption-Desorption Studies Performed by the WRIT Program." In The Technology of High-Level Nuclear Waste Disposal, Vol. 1, pp. 203-254. DOE/TIC-621, Technical Information Center, U.S. Department of Energy, Oak Ridge, Tennessee.

Simmons, C. S., C. T. Kincaid, and A. E. Reisenauer. 1986. A Simplified Model for Radioactive Contaminant Transport: The TRANSS Code. PNL-6029, Pacific Northwest Laboratory, Richland, Washington.

U.S. Department of Energy (DOE). 1987. Disposal of Hanford Defense High-Level, Transuranic and Tank Wastes. Final Environmental Impact Statement. DOE/EIS-0113, Vol. 1-5, Assistant Secretary for Defense Programs, Washington, D.C.

U.S. Department of Energy. 1989. Decommissioning of Eight Surplus Production Reactors at the Hanford Site, Richland, Washington. Draft Environmental Impact Statement. DOE/EIS-0119D, Washington, D.C.

U.S. Department of Energy (DOE). 1990a. Radioactive Waste Management. DOE/RL 5820.2A, Richland, Washington.

U.S. Department of Energy (DOE). 1990b. Low-Level Burial Grounds Dangerous Waste Permit Application; Request for Exemption from Lined Trench Requirements for Submarine Reactor Compartments. DOE/RL-88-20, Supplement 1, Richland, Washington.

van Genuchten, R. 1978. Calculating the Unsaturated Hydraulic Conductivity with a New Closed-Form Analytical Model. Water Resources Program, Department of Civil Engineering, Princeton University, Princeton, New Jersey.

van Genuchten, M. Th. 1985. RETC.F77: A Program to Analyze Observed Soil Water Tension and Hydraulic Conductivity Data. U.S. Salinity Laboratory Special Report, Riverside, California.

Woodruff, R. K. and R. W. Hanf. 1991. Hanford Site Environmental Report for Calendar Year 1990. PNL-7930. Pacific Northwest Laboratory, Richland, Washington.

**END**

**DATE  
FILMED**

3 / 22 / 93

